PRESERVATION OF MISSOURI TRANSPORTATION INFRASTRUCTURES

VOL I: Bridge Design & Load Rating

VALIDATION OF FRP COMPOSITE TECHNOLOGY
THROUGH FIELD TESTING

Strengthening of Bridge T-0530
Crawford County, MO

Prepared for:
Missouri Department of Transportation
University of Missouri-Rolla
(Project Code R03MO2-1)

February 19, 2004

TABLE OF CONTENTS

LIST OF TABLES

LIST OF FIGURES

A. INTRODUCTION

A.1 General Description

In the following report, the analysis and design procedures used in the upgrade of the load-posted Bridge T-0530, located in Crawford County, MO are summarized. Figure 1 shows a picture of the bridge. The total bridge length is *237 ft* and the total width of the deck is *23 ft*.

Figure 1 – Bridge T-0530

The structure has five equally spaced spans and each of them consists of four reinforced concrete (RC) girders monolithically cast with a *6 in.* slab, as depicted in Figure 2. Each span is provided with one transversal beam of the same depth as the main girders.

Figure 2 – Superstructure of the Bridge

A.2 Objectives

The objective of this document is to provide an analysis of the structure and the design calculations for its strengthening using externally bonded FRP (Fiber-Reinforced Polymer) systems. The FRP systems consist of FRP pre-cured laminate and FRP laminates to be installed by manual lay-up. The pre-cured laminates will be used exclusively for flexural reinforcement while the laminates will be used for both flexural reinforcement and as U-wraps for shear strengthening.

A.3 Assumptions

The following assumptions are made:

a) Nominal material properties for steel and concrete. At the onset of the project, existing material properties were validated in the field by extracting two concrete cores and a steel bar sample. The resulting values are: $f'_c=6250\ psi$ and $f_y=40\ ksi$.
b) Load configurations and analysis are consistent with AASHTO[1] Specifications; and
c) Design of the strengthening system is in compliance with ACI 440.2R-02[2] where applicable

B. STRUCTURAL ANALYSIS

B.1 Load Combinations

For the structural analysis of the bridge, definitions of the design truck load and load lane are necessary, as well as the transversal load distribution. These issues will be discussed in the next two sections. A plan view of the bridge piers and abutments is shown in Figure 3.

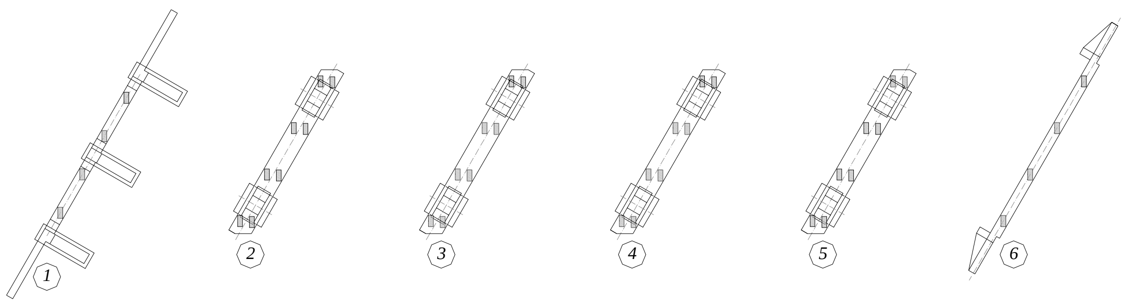

Figure 3 – Plan View of the Bridge (Not to scale)

Ultimate values of bending moment and shear force are obtained by multiplying their nominal values by the dead and live load factors and by the impact factor according to AASHTO Specifications as shown in Eq.(1):

$$\omega_u = 1.3\left[\beta_d D + 1.67(L + I)\right] \tag{1}$$

where D is the dead load, L is the live load, $\beta_d = 1.0$ as per AASHTO Table 3.22.1A, and I is the live load impact calculated as follows:

$$I = \frac{50}{L + 125} = \frac{50}{47.5 + 125} = 0.29 \leq 30\% \tag{2}$$

and $L = 47.5\ ft$ represents the span length from center-to-center of support.

B.2 Design Trucks and Load lanes

The analysis of the bridge is carried out for an HS20-44 truck load (which represents the AASHTO design truck load) and for a 3S2 truck load as requested by MoDOT, having geometrical characteristics and weight properties as shown in Figure 4.
According to AASHTO Section 3.6.3, roadway widths between *20.0* and *24.0 ft* shall have two design lanes, each equal to one-half of the roadway width.

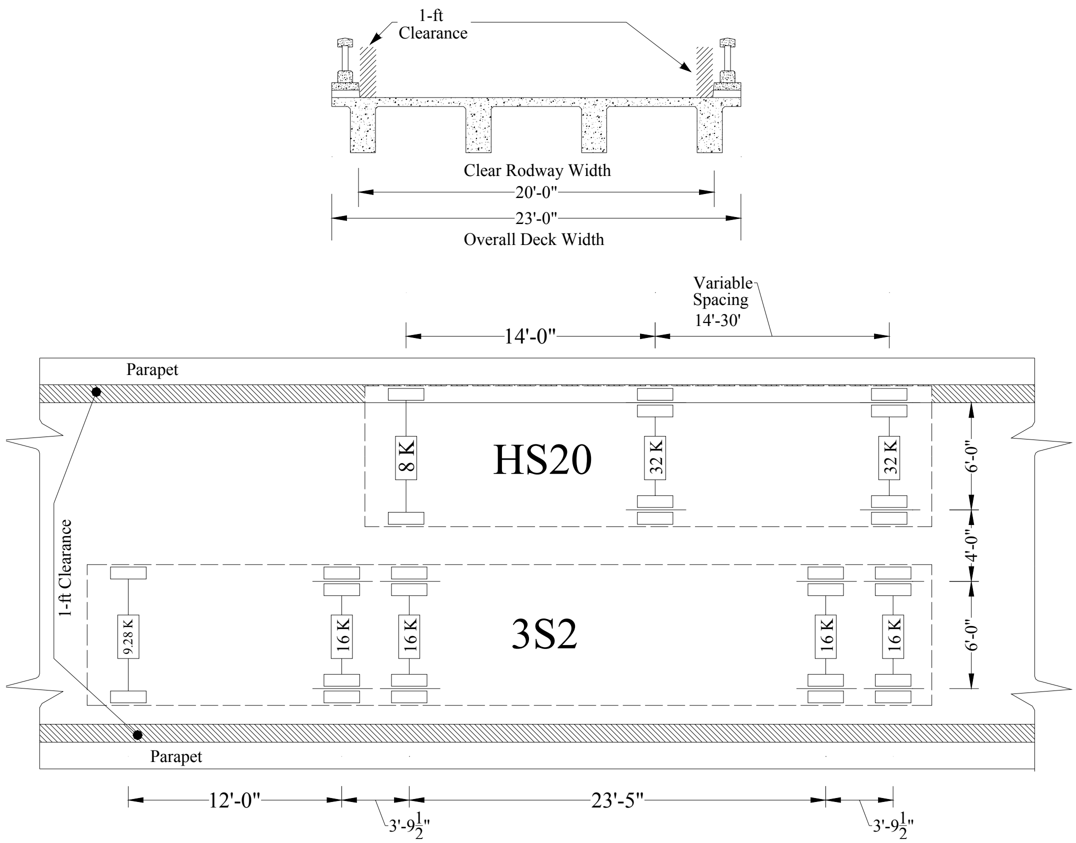

Figure 4 – Truck Load and Design Lanes

Note that the centerline of the wheels of the rear axle shown in Figure 4 is located *1.00 ft* apart from the curb as specified in AASHTO for slab design.

Three loading conditions are required to be checked as laid out in Figure 5

The HS20-44 design truck load (Figure 5*a*) has a front axle load of *8.0 kip*, second axle load, located *14.0 ft* behind the drive axle, of *32.0 kip*, and rear axle load also of *32.0 kip*. The rear axle load is positioned at a variable distance, ranging between *14.0* and *30.0 ft*. Given the specific bridge geometry, the worst loading scenario is obtained for the minimum spacing of *14.0 ft* between the two rear axles.

The 3S2 design truck load has five axles; the front axle of 9.*28 kip*, the second double axle, located *12.0 ft* behind the drive axle, of *16.0 kip*, and the rear double axle also of *16.0 kip*, as shown in Figure 5*b*. Distances between axles are given in the figure.

The load lane loading condition consists of a load of 640 lbs per linear foot, uniformly distributed in the longitudinal direction with a single concentrated load so placed on the span as to produce maximum stress. The concentrated load and uniform load is considered to be uniformly distributed over a *10'-0"* width on a line normal to the center lane of the lane. The intensity of the concentrated load is represented in Figure 5*c* for both bending moments and shear forces. This load shall be placed in such positions within the load lane as to produce the maximum stress in the member.

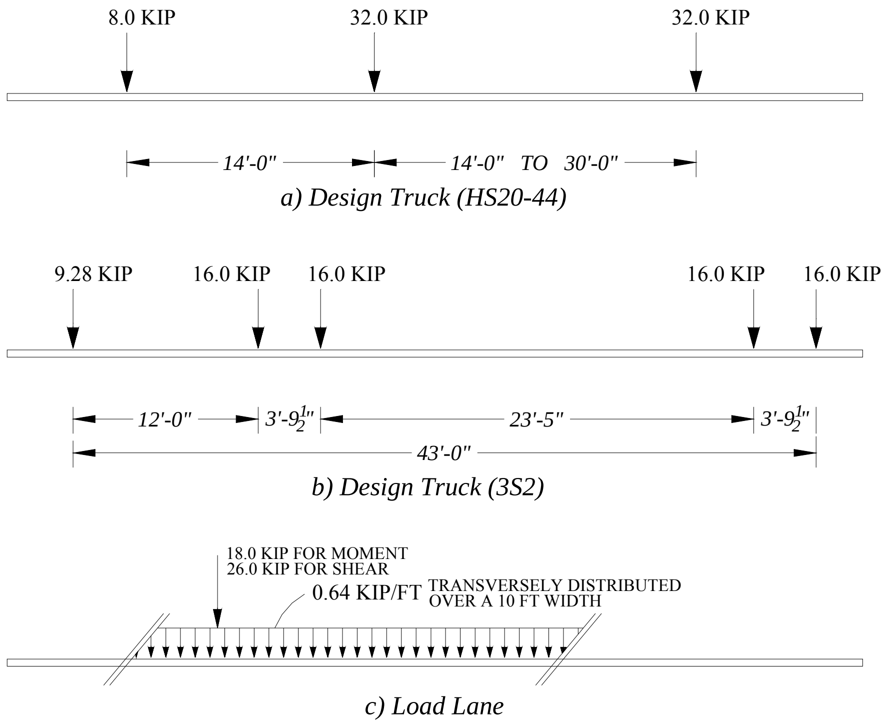

Figure 5 – Loading Conditions

B.3 Slab Analysis

The deck slab is considered to be a one-way slab system due to its large aspect ratio (panel length divided by the panel width). The width of the slab strip to be used in the analysis and design is provided by AASHTO[3] (Table 4.6.2.1.3-1) and, for cast-in-place concrete, may be written as follows for positive and negative moment regions, respectively:

$$\begin{aligned} b^{+} &= 26.0 + 6.6S \quad in. \\ b^{-} &= 48.0 + 3.0S \quad in. \end{aligned} \tag{3}$$

where S represents the center-to-center spacing of the girders *(ft)*.

A generic slab-girder system displaces as shown in Figure 6*a*. This displacement can be seen as the superposition of the displacement associated with local effects represented in Figure 6*b* and the global effect due to the vertical displacement of the girders. Since the local effect is usually significantly greater than the global effect, the latter will be neglected, and the strip analyzed using classical beam theory, assuming that the girders provide rigid support.

The analysis of the slab is carried out on a structure similar to that shown in Figure 6*b)*.

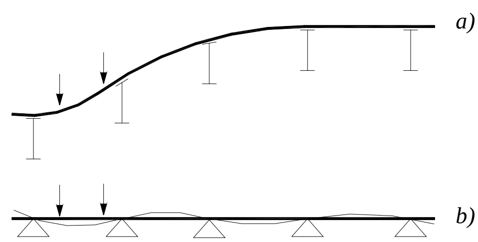

Figure 6 – Slab Deck Deflection due to External Loads

B.3.1 Results of the Analysis

In the following, only the results will be presented. A detailed protocol analysis is shown in APPENDIX A and APPENDIX B.

The four loading conditions being considered are represented in Figure 7. The first two loading conditions, *I)* and *II)*, are related to the design truck load. Loading conditions *III)* and *IV)* of Figure 7 refer to the load lane.

Table 1 summarizes the results in terms of ultimate (factored) bending moments and shear forces for the case of wheel loads corresponding to the HS20-44 truck load, which represents the most demanding loading condition. The values are adopted for design.

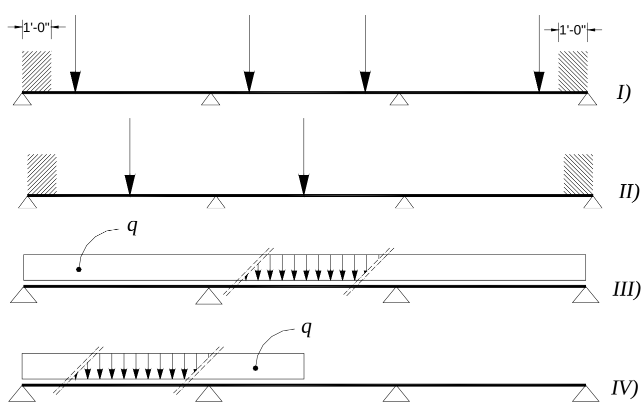

Figure 7 – Loading Conditions for Slab Analysis

Figure 8 shows the bending moment diagrams due to the live load only as the design truck load moves transversally on the bridge deck for both loading condition *I)* and *II)*, respectively. These moments were divided by the strip widths shown in Eq. (3) to obtain the values of unit moment summarized in Table 1. Values of Table 1 do take into account the moment due to the dead load as well.

Table 1 – Slab Ultimate Bending Moments and Shear Forces

Loading Condition	Number of Design Lanes	Moment Redistribution *a)*	Positive Moment*b)* (k-ft/ft)	Negative Moment*c)* (k-ft/ft)	Shear*c)* (kip/ft)
I)	2	Before redistribution	9.1	5.9	9.4
		After redistribution	11.0	4.7	
II)	1	Before redistribution	9.2	6.1	8.3
		After redistribution	11.1	4.9	
III)	2	Before redistribution	1.5	1.8	1.7
IV)	1	Before redistribution	1.8	1.4	2.8

a) Moment redistribution is carried out according to ACI 318-99, Appendix B, Section B.8.4.3
b) Computed close to mid-span depending on load location (See Figure 8)
c) Computed at a cross-section flush with the girder

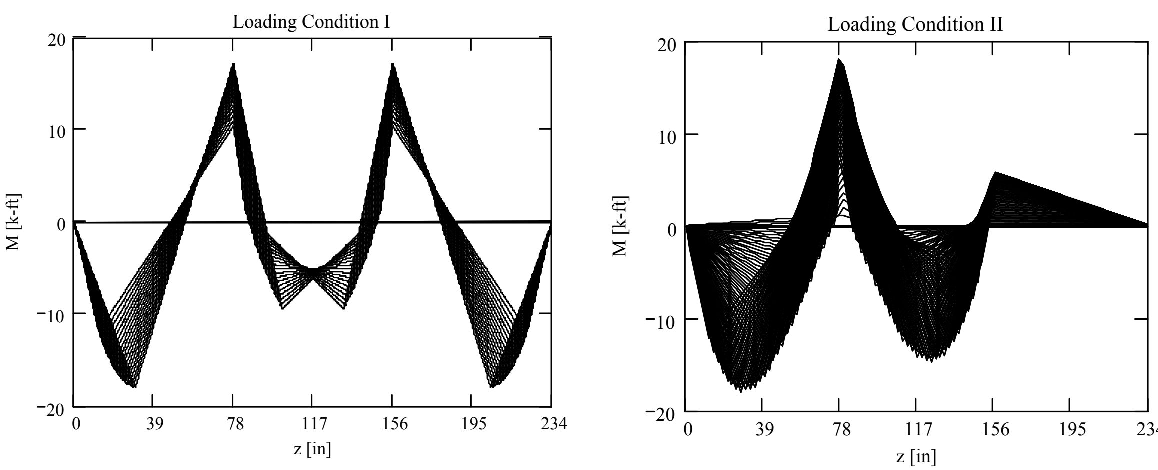

Figure 8 – Bending Moment Diagram Envelopes

B.4 Transversal Load Distribution to Girders

B.4.1 Model for Computing Distribution

According to the truck load arrangement of Figure 4, the transversal load distribution can be found by analyzing the structures in Figure 9, where a generic axle of unit weight *P* has been assumed. Because of geometrical restraints, the truck can not drive on the overhang; hence, the small cantilever portion of the deck has been neglected.

By increasing the value of *x* represented in Figure 9, the design lane(s) move from the left to the right portion of the bridge deck. As this movement is allowed, two possible different loading configurations can be recognized.

The difference between these configurations is related to the number of wheels per bay, as summarized in Table 2. Any other loading condition can be represented by reference to one of the two aforementioned conditions. Table 2 summarizes the values obtained from Figure 9 for the bridge under examination.

A complete analysis of the conditions represented in Figure 9 is carried out according to the protocol of APPENDIX A. In the following, only the results of this analysis are presented.

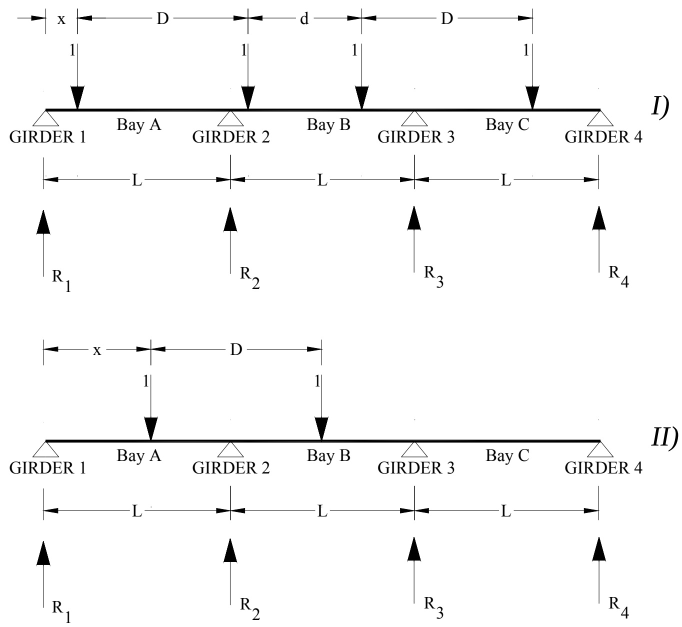

Figure 9 – Transversal Load Distribution and Loading Conditions

Table 2 – Loading Conditions and Bridge Dimension

Loading Condition	Reference	Bay A	Bay B	Bay C	*x* (in)	*D* (in)	*d* (in)	*L* (in)
I	Figure 9-*I)*	1 wheel	2 wheels	1 wheel	$12 \leq x \leq 30$	72	48	78
II	Figure 9-*II)*	1 wheel	1 wheel	0 wheel	$12 \leq x \leq 78$			

B.4.2 Results of the Analysis

Figure 10 shows the load lane conditions when two and one design lane are considered. The calculations related to this analysis are summarized in APPENDIX B.

Figure 11 shows each reaction $R_1 \ldots R_4$ of Figure 9 (which represents the load carried by each girder) as a function of x.

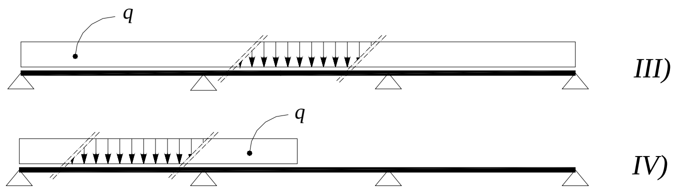

Figure 10 – Transversal Load Distribution: Load Lane Analysis

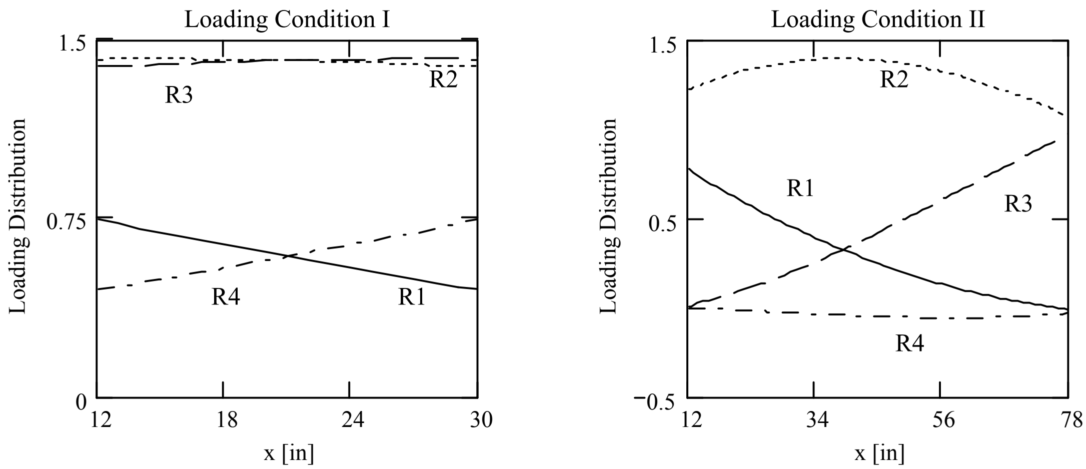

a) Loading Condition I) *b) Loading Condition II)*

Figure 11 – Reactions as a Function of *x*

Table 3 summarizes the findings of the distribution of the load to the girders. The k_L coefficients represent the multiplier of the load to be used in the girder analysis.

Table 3 – Vertical Reactions; k_L Coefficients

Coefficients	Loading Condition	Exterior Girders		Interior Girders	
		R1	R4	R2	R3
k_L	*I)*	0.746	0.746	1.420[a)]	1.420
	II)	0.775[a)]	-0.057	1.394	0.974
	III)	0.40	0.40	1.10[b)]	1.10
	IV)	0.403[b)]	-0.004	1.064	0.037

a) Design values to be used for the design truck analysis of the girders
b) Design values to be used for the load lane analysis of the girders

B.5 Girders Analysis

B.5.1 Model for Computing Internal Forces and End Reactions

The analysis is conducted for the three loading conditions recognized in Figure 5 namely: *1)* HS20-44 truck load, *2)* 3S2 truck load, and 3*)* load lane.

B.5.1.1 Load Lane Analysis

In the last loading condition of Figure 5*c)*, a uniform load of *0.64 kip/ft* is distributed over the entire length of the girder. Transversely, it is assumed to be uniformly distributed over a *10 ft* width. Hence, the portion of the uniformly distributed load, q, carried by each of the four girders can be expressed as follows:

$$q = (0.64)k_L \tag{4}$$

where k_L represents the fraction of the total load carried by each individual girder. The value of k_L for interior and exterior girders is reported in Table 3.

The analysis related to the concentrated load being part of the load lane is reported in APPENDIX B.

B.5.1.2 HS20-44 and 3S2 Analysis

Figure 12 shows a generic girder with a generic truck load moving on it as the value of x_1 increases from *0* to *L*.

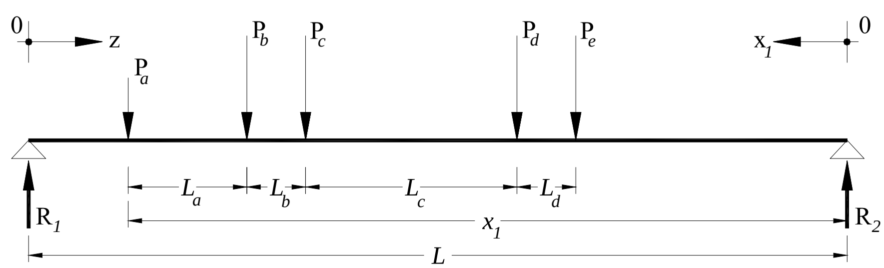

Figure 12 – Design Truck Load on the Girder

The values of P_i *(i=a,b,c,d,e)* can be expressed as follows:

$$P_i = P_{wi} k_L \tag{5}$$

where P_{wi} is the wheel load defined by AASHTO (*4* and *16 kip*, for an HS20-44 truck load, and *4.64* and *8 kip* for a 3S2 truck load) and k_L represents the fraction of the total load carried by each individual girder. The determination of k_L is presented in APPENDIX A and its value is summarized in Table 3 for interior and exterior girders, respectively.

Table 4 summarizes values reported in Figure 12 and Figure 5*c)* for the girder under examination and for the three loading conditions being considered.

As the design truck load moves from the right to the left side of the girder, five different loading conditions are recognized, as shown in Figure 13.

A complete structural analysis protocol for an HS20-44 design truck load is carried out in APPENDIX C.

Table 4 – Parameters for Girder Analysis

Analysis Type	x_1 (ft)	L_a (ft)	L_b (ft)	L_c (ft)	L_d (ft)	L (ft)	P_{wa} (kip)	P_{wb} (kip)	P_{wc} (kip)	P_{wd} (kip)	P_{we} (kip)
HS20-44	Varies	14.0	14.0	0.0	0.0	45.8	4.0	16.0	16.0	0.0	0.0
3S2	Varies	12.0	3.8	23.4	3.8	45.8	4.64	8.0	8.0	8.0	8.0
Load lane [a)]	L/2	0.0	0.0	0.0	0.0	45.8	18.0 [b)]	0.0	0.0	0.0	0.0
	d[d)]	0.0	0.0	0.0	0.0	45.8	26.0 [c)]	0.0	0.0	0.0	0.0

Notes: *a)* Related to the concentrated load only; *b)* For bending moment analysis; *c)* For shear force analysis; *d)* Girder effective depth

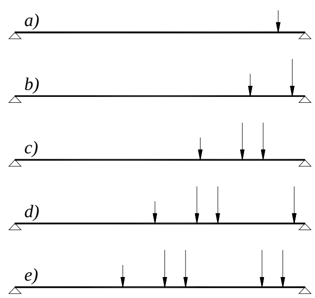

Figure 13 – Design Truck: Possible Loading Conditions

B.5.2 Moment and Shear due to Design Trucks

In the following, only the results needed for the design of critical girder cross-sections are presented. Graphical results will be presented only for the case of the design trucks HS20-44 and 3S2. Results related to the load lane analysis will be summarized later in Table 5 and Table 6.

Figure 14 and Figure 15 show the diagrams of both moments and shear forces as the design trucks move on the interior and exterior girders, respectively.

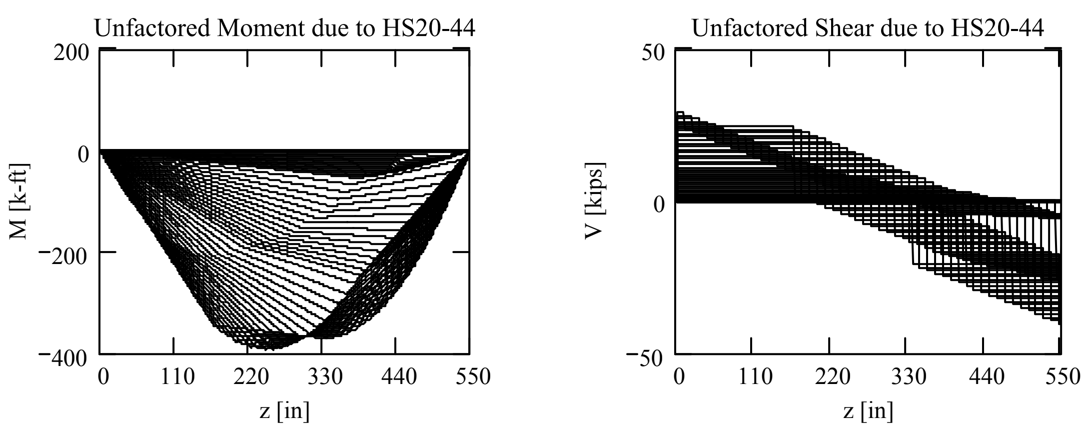

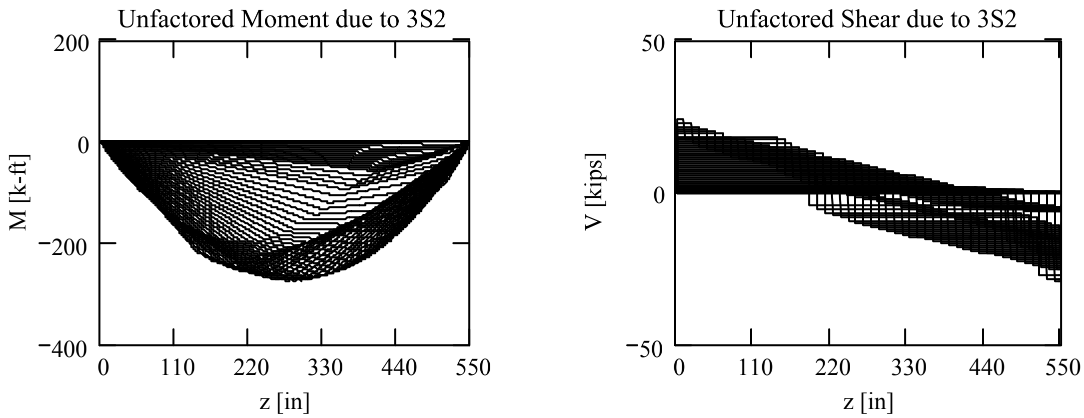

Figure 14 – Bending Moments and Shear Forces Diagrams for Interior Girders

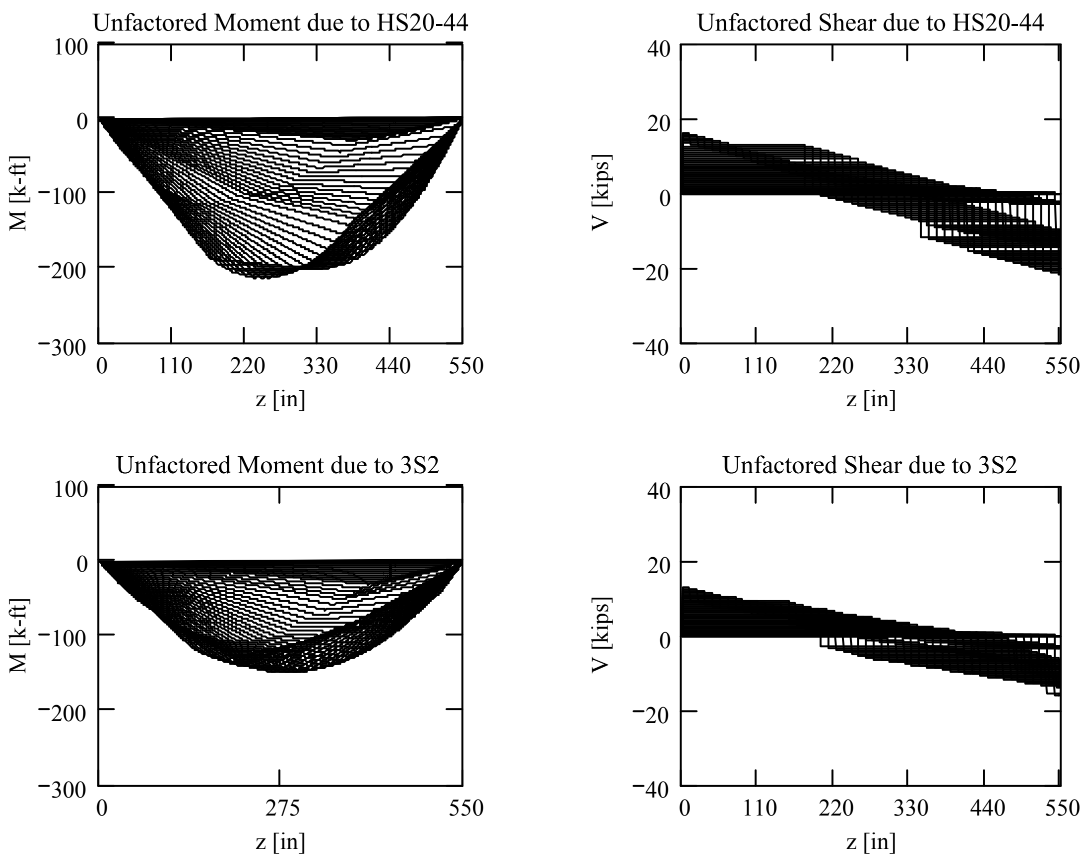

Figure 15 – Bending Moment and Shear Force Diagrams for Exterior Girders

Bending moment and shear force represented in Figure 14 and Figure 15 refer to both design trucks HS20-44 and 3S2. Ultimate values are then obtained by taking into account the load factors and by adding the moment and shear due to the dead load.

B.5.3 Load Combinations and Results

Ultimate bending moments and shear forces calculated at several cross-sections, either at a distance *X* (for moment) or *v* (for shear) from the support (see Figure 16), are summarized in Table 5 and Table 6 for both HS20-44 Design truck load and load lane. The other loading condition (3S2 design truck load) is not presented because it does not control the design as already shown in Figure 14 and Figure 15. The reported values account for both factored dead and live load.

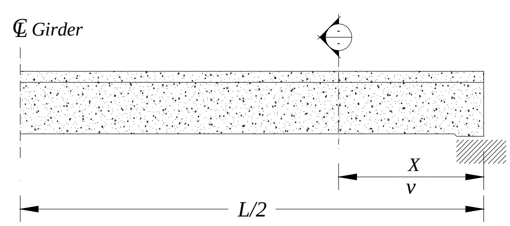

Figure 16 – Identification of Girders' Cross-Sections

The cross-sections indicated in Table 5 and Table 6 (i.e, 1-1, A-A etc.) were shown to be critical locations in a preliminary analysis.

Table 5 – Breakdown of Moment at Critical Cross-Sections (k-ft)

Span	Girder	Section		Dead Load	Live Load		Factored Load	
		Description	*X* (in.)		HS20-44	Lane	HS20-44	Lane
All	Exterior	Support	0	0	0	0	0	0
		1-1	44.25	135.9	73.6	53.2	382.8	325.6
		2-2	83.25	236.0	124.7	97.2	656.0	578.8
		3-3	120	313.4	161.3	136.2	859.1	788.4
		4-4	156	373.3	185.9	172.0	1005.9	966.5
		5-5	204	428.7	206.6	216.2	1135.9	1162.0
		Mid-span	275	459.3	214.4	273.9	1197.5	1363.3
	Interior	Support	0	0	0	0	0	0
		1-1	44.25	107.8	134.8	87.8	514.8	386.0
		2-2	83.25	187.2	228.6	157.3	878.6	683.7
		3-3	120	248.6	295.5	216.0	1144.3	927.7
		4-4	156	296.1	340.5	267.1	1331.1	1132.4
		5-5	204	340.0	378.5	325.3	1493.9	1352.5
		Mid-span	275	364.3	392.9	390.8	1574.0	1567.4

Table 6 – Breakdown of Shear at Critical Cross-Sections (kip)

Span	Girder	Section		Dead Load	Live Load		Factored Load	
		Description	v (in.)		HS20-44	Lane	HS20-44	Lane
All	Exterior	Support	0	40.1	22.0	30.3	113.7	137.1
		A-A	83.25	28.0	18.0	5.7	86.7	52.2
		B-B	108	24.3	16.7	5.1	78.4	46.0
		C-C	144	19.1	14.9	4.4	66.6	37.0
		D-D	204	10.3	11.9	3.1	46.8	22.0
		E-E	240	5.1	9.8	2.3	34.1	13.1
		Mid-span	275	0	8.0	1.6	22.4	4.3
	Interior	Support	0	31.8	40.2	40.6	153.0	154.9
		A-A	83.25	22.2	32.9	12.8	120.2	64.6
		B-B	108	19.3	30.6	11.3	110.1	56.8
		C-C	144	15.1	27.3	9.2	95.6	45.5
		D-D	204	8.2	21.7	5.7	71.0	26.6
		E-E	240	4.0	17.9	3.6	55.0	15.3
		Mid-span	275	0	14.7	1.5	40.8	4.3

B.6 Bent Analysis

B.6.1 Model for Computing Internal Forces

The bent cap can be analyzed as a portal frame. The worst loading condition imposed on the bent from the superstructure is shown in Figure 17 for bents 2 through 5 (see Figure 3). The two vertical reactions R_1 and R_2 for both interior and exterior girders are shown in Figure 18 for an HS20-44 truck load as a function of x_1.

Note that the values of x_1 shown in Figure 18 represent the worst loading scenario.

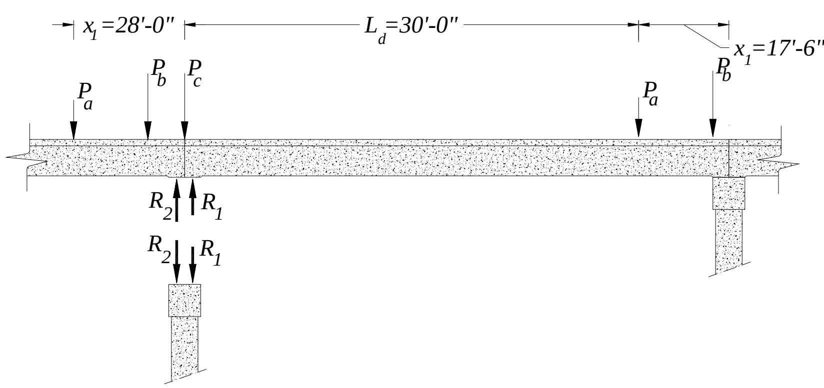

Figure 17 – Bent Loading Condition

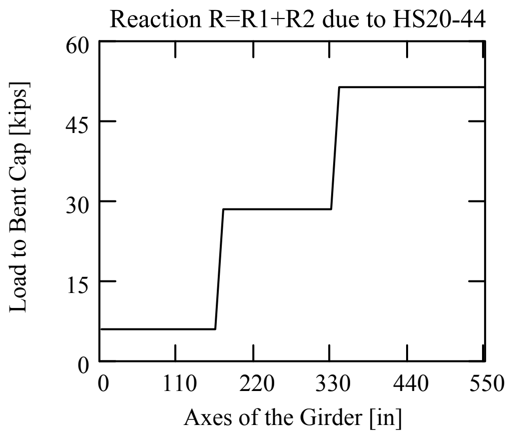

a) Interior Girders, R_{Int}

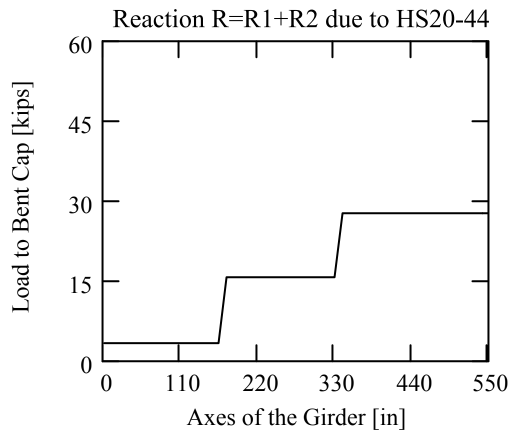

b) Exterior Girders, R_{Ext}

Figure 18 – Reactions R for Interior and Exterior Girders

Bent analysis is carried out considering the structure shown in Figure 19. Vertical loads P_1 and P are calculated as follows:

$$\begin{aligned} P_1 &= 1.3R_{DExt} + (1.3)(1.67)(1.29)R_{Ext} \\ P &= 1.3R_{DInt} + (1.3)(1.67)(1.29)R_{Int} \end{aligned} \tag{6}$$

where R_D is the vertical reaction due to the dead load of girders and deck, and subscripts *Ext* and *Int* refer to exterior and interior girders, respectively. From Figure 18*a* and *b*, the maximum values of the vertical reactions may be calculated as $R_{Int}=51.1$ and $R_{Ext}=27.7$ *kip*. The reactions due to dead load for both girders can be taken from previous sections related to the girder analysis as $R_{DInt}=31.7$ and $R_{DExt}=41.5$ *kip* for internal and external girders, respectively. Finally, $P_1=131.5$ *kip* and $P=184.3$ *kip*.

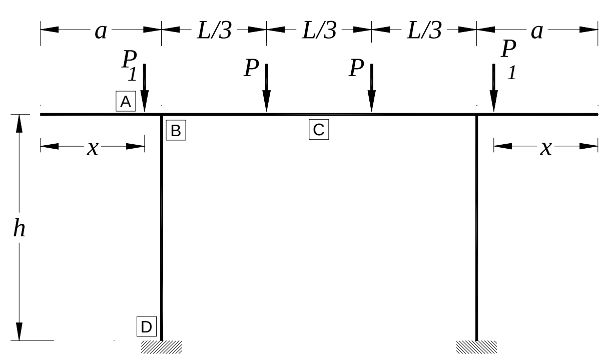

Figure 19 – Bent Frame

B.6.2 Load Combination and Results

Bending moment and shear force diagrams for this loading condition are shown in Figure 20. A detailed calculation protocol is provided in APPENDIX D. Table 7 summarizes ultimate moments and shear forces calculated using Eq. (1) at five cross-sections where maximum values are reached.

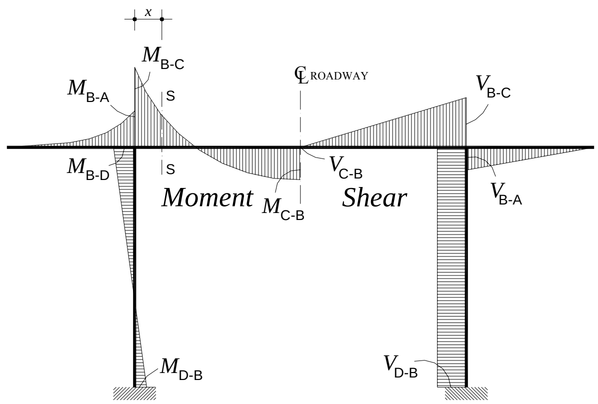

Figure 20 – Bending Moment and Shear Force Diagram

Table 7 – Ultimate Moment and Shear

Section	M_u (k-ft)	V_u (kip)
B-A	309.0	131.5
B-C	564.5	184.3
C-B	495.2	0
B-D	255.5	39.1
D-B	127.8	39.1

In Table 7 only the results corresponding to the live load are presented because the contribution of the self weight of the member can be neglected.

The bending moment due to live load in a generic cross-section *S-S* located at a distance *x* from the centerline of the pier (see Figure 20) can be expressed as follows:

$$M_{S-S} = M + M_1 - M_2 - 2Px \tag{7}$$

The meanings of the symbols presented in Eq. (7) are reported in APPENDIX D.

C. DESIGN

C.1 Assumptions

Strengthening design is carried out according to the principles of ACI 440.2R-02 (ACI 440 in the following). The properties of concrete, steel, and FRP laminates used in the design are summarized in Table 8. The reported FRP properties are guaranteed values. The FRP systems used in the design of this bridge are highlighted in Table 8.

The ϕ factors used to convert nominal values to design capacities are obtained as specified in AASHTO for the as-built and from ACI 440 for the strengthened members.

Table 8 – Material Properties

Concrete Compress. Strength f'_c (psi)	Steel Yield Strength f_y (ksi)	FRP Type			FRP Tensile Strength f^*_{fu} (ksi)	FRP Modulus of Elasticity E_f (ksi)	FRP Size or Thickness t_f (in)
		NSM System	Manual Lay-up	Pre-cured Laminate			
6,250[a)]	40	Type-1*a*	-	-	300	19,000	0.079x0.63
		Type-1*b*	-	-	300	19,000	4/8 bar size
		-	Type-2	-	550	33,000	0.0065
		-	-	Type-3	350	20,000	0.0787

a) From testing of concrete cores

Material properties of the FRP reinforcement reported by manufacturers, such as the ultimate tensile strength, typically do not consider long-term exposure to environmental conditions, and should be considered as initial properties. FRP properties to be used in all design equations are given as follows (ACI 440):

$$\begin{aligned} f_{fu} &= C_E f^*_{fu} \\ \varepsilon_{fu} &= C_E \varepsilon^*_{fu} \end{aligned} \tag{8}$$

where f_{fu} and ε_{fu} are the FRP design tensile strength and ultimate strain considering the environmental reduction factor *(C_E)* as given in Table 7.1 (ACI 440), and f^*_{fu} and ε^*_{fu} represent the FRP guaranteed tensile strength and ultimate strain as reported by the manufacturer (see Table 8). The FRP design modulus of elasticity is the average value as reported by the manufacturer.

C.2 Slab Design

C.2.1 Assumptions

Slab geometrical properties and internal steel flexural reinforcement are summarized in Figure 21 and Table 9.

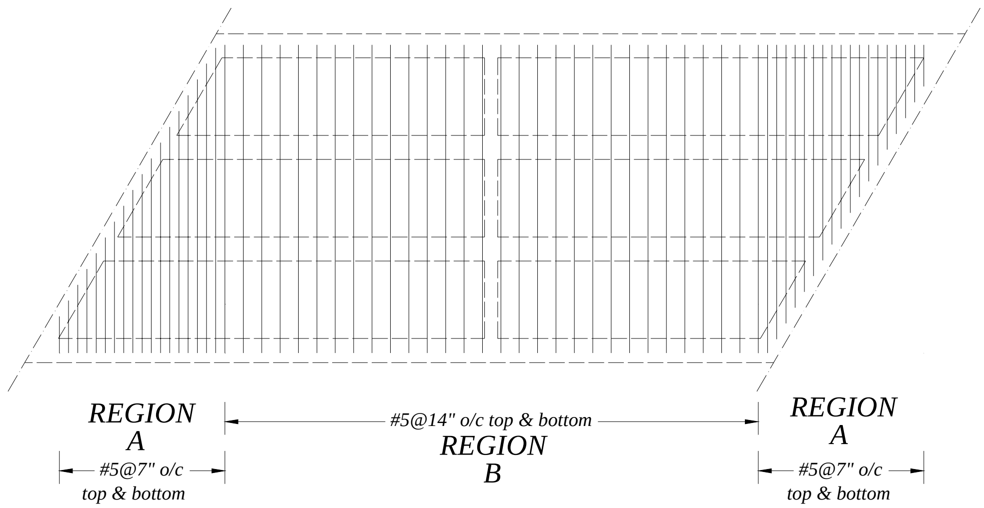

Figure 21 – Slab Internal Steel Reinforcement

Table 9 – Slab Geometrical Properties and Internal Steel Reinforcement

Region	Slab Thickness H (in)	Width of the Web b (in)	Tensile Steel Area A_s (in^2/ft)	Effective Depth d (in)	Compression Steel Area A'_s (in^2/ft)	Effective Depth d' (in)
A-A	6	12	0.53	5.0	0.53	1.0
B-B	6	12	0.27	5.0	0.27	1.0

C.2.2 Positive Moment Strengthening

For the two regions being considered (A-A, and B-B), the strengthening recommendations summarized in Table 10 are suggested for the case of mid-span location (maximum positive moment).

When adding FRP, the failure mode is usually governed by FRP rupture because of its limited ultimate strain at failure as compared to that of steel. This also represents an optimal use of an expensive material. Only when the number of applied FRP plies becomes larger, will the failure mode change from tension controlled (FRP rupture) to concrete crushing.

Slab flexural strengthening of the positive moment region is shown in Figure 22 and Figure 23. Figure 24 shows span definition and strengthening material used.

Table 10 – Slab Positive Moment Capacity

Pre-cured Laminate	Section	Strengthening Scheme	Failure Mode	ϕM_n (k-ft/ft)	M_u (k-ft/ft)
Type-2	A-A	No FRP	CC	8.3	11.1
		1 Ply, 4" wide @12" ocs	TC	11.8	
	B-B	No FRP	CC	4.6	
		1 Ply, 9" wide @15" ocs	TC	11.1	
Type-3	A-A	No FRP	CC	8.3	
		1 Plate, 3" (80 mm) wide @18" ocs	TC	12.9	
	B-B	No FRP	CC	4.6	
		1 Plate, 3" (80 mm) wide @15" ocs	TC	11.2	

CC=Concrete Crushing, TC=Tension Controlled.

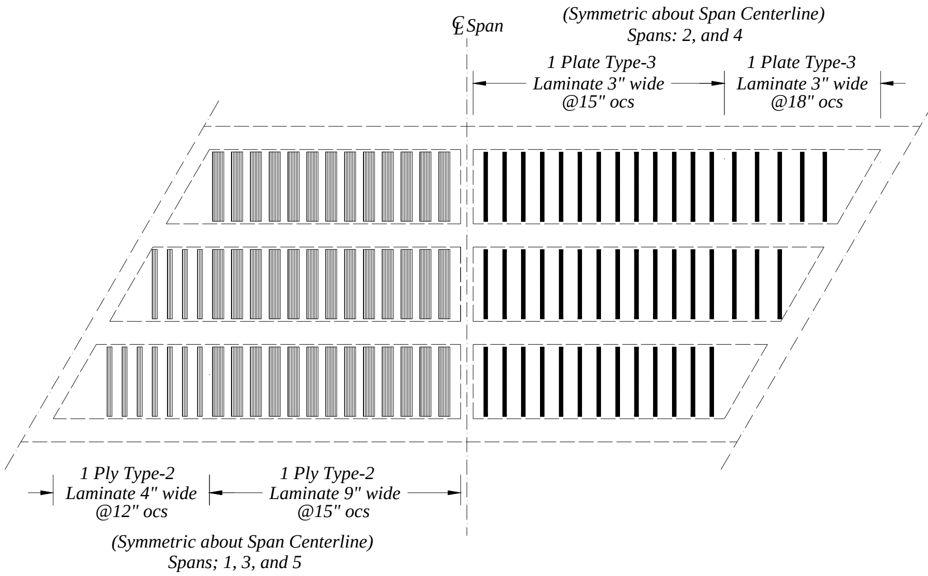

Figure 22 – Plan View of Slab Strengthening

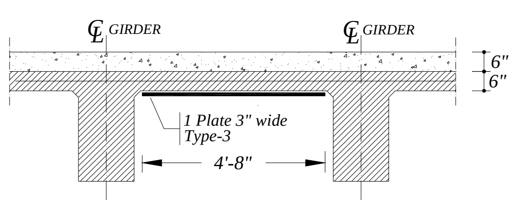

Figure 23 – Slab Cross-Section thru Span 2 and 4

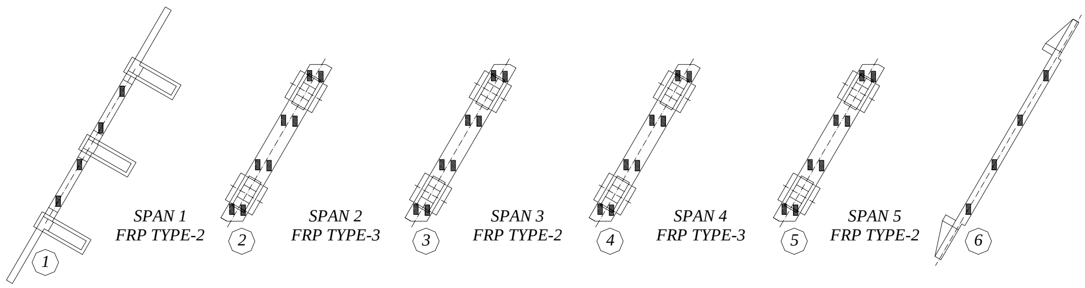

Figure 24 – Slab Definition and Strengthening Material Used

C.2.3 Negative Moment Check

Strengthening of the negative moment region of the bridge deck is not a viable solution. The as-built negative moment capacity is summarized in Table 11. Both sections A-A and B-B (see Figure 21) do not need any flexural strengthening because their as-built capacity is acceptable.

Table 11 – Slab Negative Moment Capacity (k-ft/ft)

Region	Failure Mode	ϕM_n	M_u
A-A	CC	8.3	4.9
B-B	CC	4.6	

CC=Concrete Crushing

It is to be noted that both positive and negative moment acting on the deck have been calculated using the center-to-center distance between supports. AASHTO Section 3.24.1.1 allows the use of a smaller span length $(L_{net}+2h_s)$ that further reduces both positive and negative flexural demand.

C.2.4 Shear Check

Shear strengthening of slab-deck systems is not a viable solution. The as-built shear capacity is summarized in Table 12. No shear strengthening will be provided on the slab since the values of the as built shear capacity and demand are sufficiently close.

Table 12 – Slab Shear Capacity

Region	ϕV_n (kip)	V_u (kip)
A-A	8.8	9.4
B-B	8.2	

Table 12 reports data for V_u computed considering the resultant load from each set of two tires. Since each tire has a width of *20 in.* (AASHTO Section 3.30), the distributed load would have a total width of *4x20=80 in.* over a span of 78 *in*. If one were to consider this load uniformly distributed over the entire width of the deck, the equivalent load per linear foot would be $q=0.875$ *kip/ft*, which would correspond to an ultimate shear computed at the same location of Table 12 of $V_u=7.6$ *kip/ft*. This value represents a lower bound while the one in Table 12 is the upper bound.

C.3 Girders Design

C.3.1 Assumptions

Girder geometrical properties are reported in Table 13 and Figure 25*a*; Table 14, Table 15, and Figure 25*b* and *c* summarize internal flexural and shear reinforcement at different cross-sections where there is a change in the lay-out of the reinforcement.

The expression for the flange width, b_{eff}, is given by the following equations, according to AASHTO Section 8.10.1 for interior and exterior girders, respectively:

$$\begin{aligned} b_{eff}^{Int} &= \min\left(\frac{L}{4}, 12h_s + b, S\right) \\ b_{eff}^{Ext} &= b + \min\left(\frac{L}{12}, 6h_s, \frac{S-b}{2}\right) \end{aligned} \tag{9}$$

where L is the girder length, h_s and b are defined in Table 13, and S represents the center-to-center girder spacing.

Table 13 – Geometrical Properties

Girder Type	Overall Height, h (in)	Width of the Web, b (in)	Width of the Flange, b_{eff} (in)	Slab Thickness, h_s (in)
Interior	37	17	78	6
Exterior	37	17	47.5	6

Table 14 – Flexural Internal Steel Reinforcement

Girder Type	Section (see Figure 25c)	Tensile Steel Area, A_s (in^2)	Effective Depth, d (in)	Compression Steel Area, A'_s (in^2)	Effective Depth, d' (in)
Interior/ Exterior	Support	6.25	34.5	5.23 Int / 4.56 Ext	1.5
	1-1	9.375	33.5	5.23 Int / 4.56 Ext	1.5
	2-2 to Mid-span	12.50	33.0	2.10 Int / 1.43 Ext	1.5

Table 15 – Shear Internal Steel Reinforcement

Girder Type	Section (see Figure 25*c*)	Stirrup Area A_{vs} (in^2)	Stirrups Spacing s_s (in)	Bent Bar Area A_{vb} (in^2)	Bent Bar Spacing s_b (in^2)
Interior/ Exterior	Support	0.4	9	3.125	39
	A-A	0.4	9	0	0
	B-B	0.4	12	0	0
	C-C	0.4	15	0	0
	D-D to Mid-span	0.4	18	0	0

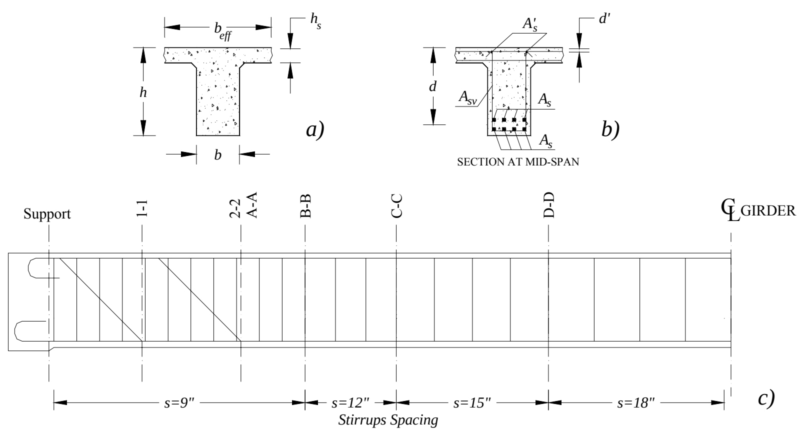

Figure 25 – Girder Dimensions and Internal Reinforcement

C.3.2 Positive Moment Strengthening

All interior and exterior girders need flexural strengthening because of the increased live load due to the revised loading condition of an HS20-44 truck load.

Table 16 summarizes the achieved flexural capacity at mid-span for interior and exterior girders as a function of the adopted strengthening scheme.

When FRP laminates are used, the bond dependent coefficient, κ_m, defined by Eq.(9-2) of ACI 440, accounts for cover delamination or FRP debonding that could occur if the force in the FRP cannot be sustained by the substrate. When FRP U-Wraps are installed to anchor the external flexural reinforcement, the value of κ_m may be increased to *0.90* since both cover delamination and FRP debonding are effectively prevented.

Figure 26 shows the flexural demand and the as built and strengthened capacities of both interior and exterior girders, respectively. The demand has been shown for the three loading conditions being studied.

Table 16 – Flexural Capacity of Interior and Exterior Girders at Mid-span

<table>
<tr><th>FRP Type</th><th>Girder Type</th><th>Description</th><th>κ_m (-)</th><th>ϕM_n (k-ft)</th><th>M_u (k-ft)</th></tr>
<tr><td rowspan="4">Type-2</td><td rowspan="2">Interior</td><td>No FRP</td><td>-</td><td>1215.6</td><td rowspan="2">1574.0</td></tr>
<tr><td>4 Plies, 16” wide</td><td>0.85</td><td>1573.7</td></tr>
<tr><td rowspan="2">Exterior</td><td>No FRP</td><td>-</td><td>1201.9</td><td rowspan="2">1363.3</td></tr>
<tr><td>2 Plies, 16” wide</td><td>0.9</td><td>1386.4</td></tr>
<tr><td rowspan="4">Type-3</td><td rowspan="2">Interior</td><td>No FRP</td><td>-</td><td>1215.6</td><td rowspan="2">1574.0</td></tr>
<tr><td>1 Plate, 12” (300mm) wide</td><td>0.85</td><td>1573.9</td></tr>
<tr><td rowspan="2">Exterior</td><td>No FRP</td><td>-</td><td>1201.9</td><td rowspan="2">1363.3</td></tr>
<tr><td>1 Plate, 12” (300 mm) wide</td><td>0.495</td><td>1386.8</td></tr>
</table>

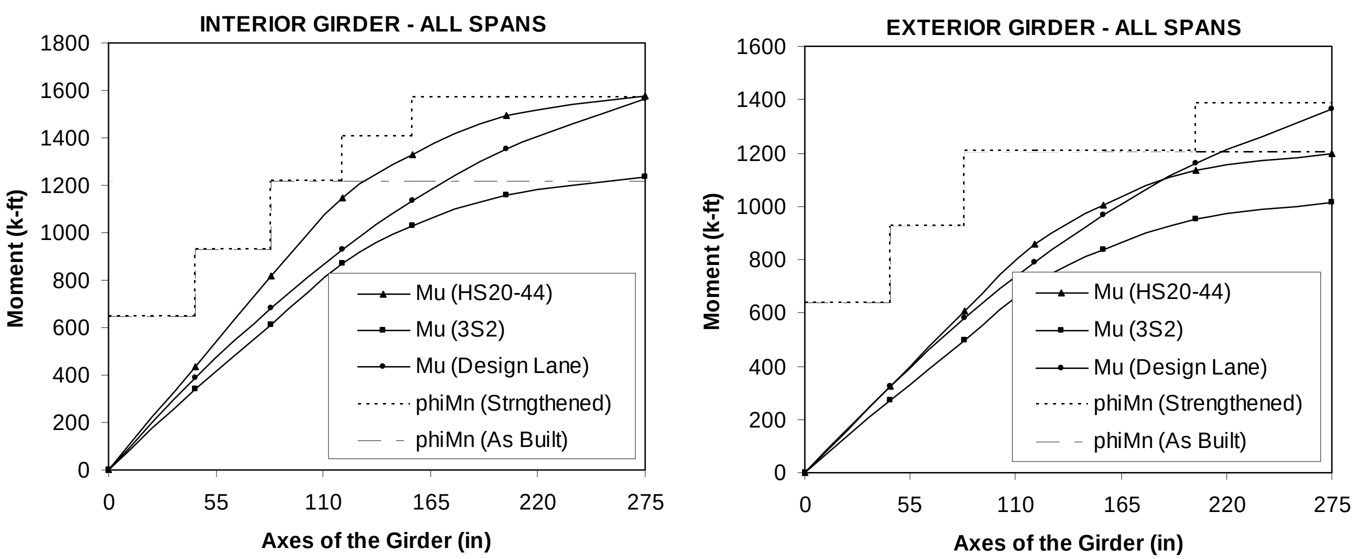

Figure 26 – Flexural Demand and Flexural Capacity

A sketch showing the layout of FRP flexural reinforcement for interior girders is presented in Figure 27 and Figure 28 for fiber Type-2 and Type-3, respectively.

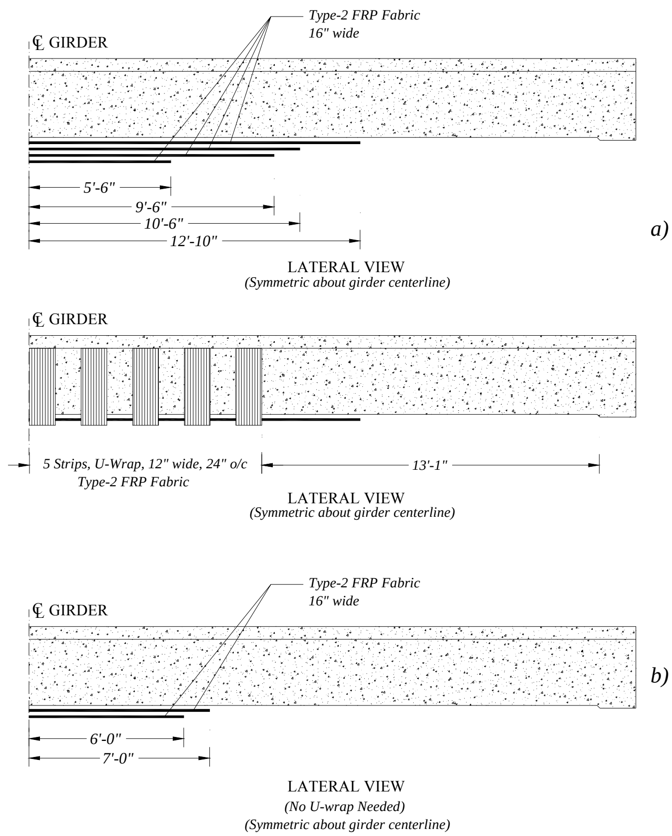

Figure 27 – Type-2 FRP Flexural Reinforcement: *a)* Interior, and *b)* Exterior Girders

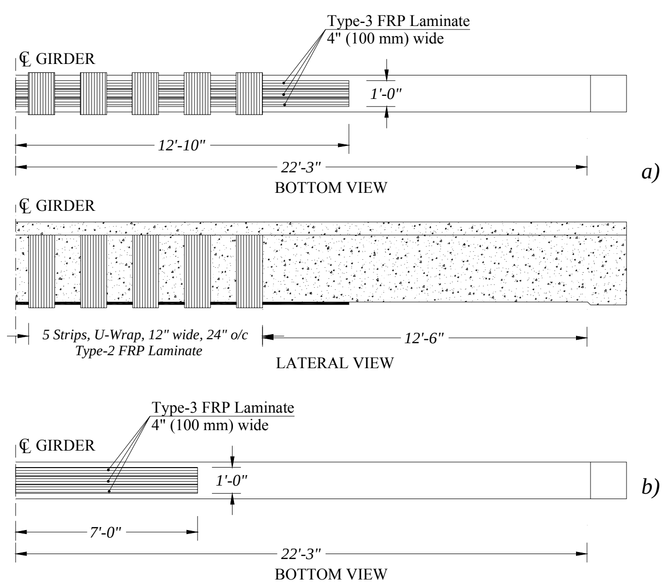

Figure 28 – Type-3 FRP Flexural Reinforcement: *a)* Interior, and *b)* Exterior Girders

As the ultimate moment decreases towards the supports, the total number of plates reduces. Figure 27*b)* shows Type-2 (See Table 8) FRP U-wraps installed by manual lay-up to hold the FRP flexural reinforcement in place.

C.3.3 Negative Moment Check

All girders are simply supported, and therefore no negative moment exists.

C.3.4 Shear Strengthening

The concrete contribution to the shear capacity has been assumed to be based on Eq. (11-5) of ACI 318-99[4] as follows:

$$V_c = \left(1.9\sqrt{f_c^{'}} + 2500\rho_w \frac{V_u d}{M_u}\right) b_w d \leq 3.5\sqrt{f_c^{'}} b_w d \tag{10}$$

where $\rho_w = A_s/b_w d$, V_u and M_u represent ultimate bending moment and shear force acting at the same cross-section, respectively, and b_w and d are width and effective depth of the girder. The steel contribution to the shear capacity can be expressed as follows:

$$V_f = \frac{A_{vs} f_y d}{s_s} + \frac{A_{vb} f_f (\sin\alpha + \cos\alpha) d}{s_b} \leq 2\frac{A_{vs} f_y d}{s_s} \tag{11}$$

where α represents the slope of the bent bar *(α=45°)*, and all other symbols are indicated in Table 15. The limitation expressed by the third term of Eq. (11) is a conservative assumption to take into account the localized effect exerted by the bent bars.

For this particular case, shear strengthening is not needed as summarized in Table 17 for both interior and exterior girders.

Table 17 – Shear Capacity at Support

Girder Type	Description	k_v (-)	ϕV_n (kip)	V_u (kip)
Interior	No Strengthening	-	193.9$^{a)}$	154.9
Exterior	No Strengthening	-	139.9$^{a)}$	137.1

a) Concrete shear contribution calculated as $V_c = 2\sqrt{f_c^{'}} b_w d$

Figure 29 shows the as-built shear capacity compared to the shear demand for the three loading conditions being studied.

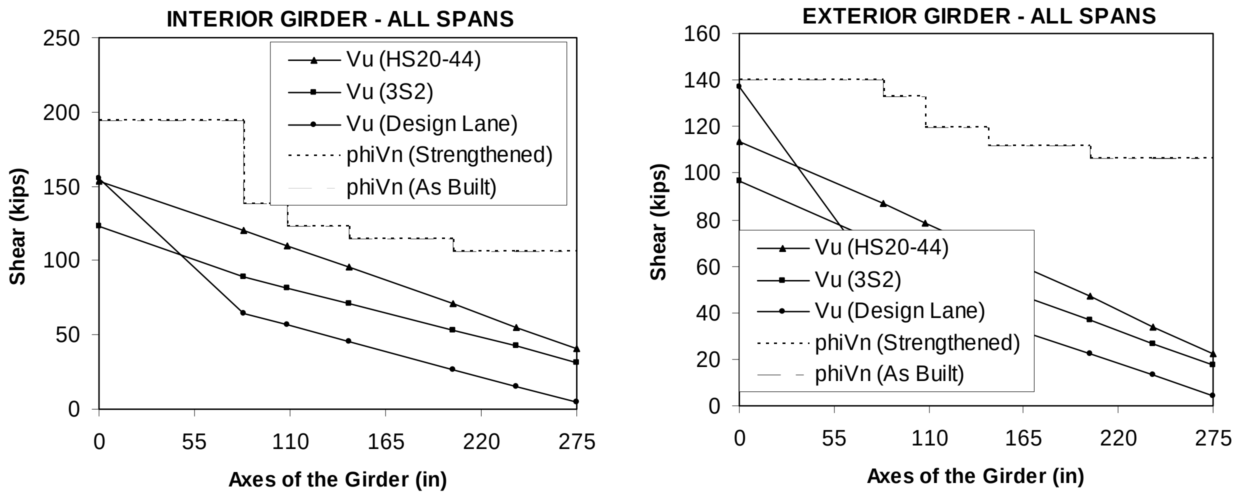

Figure 29 – Shear Demand and Shear Capacity

C.4 Bent Design

C.4.1 Assumptions

Bent geometrical properties are summarized in Table 18 and Figure 30.

Table 18 – Geometrical Properties

Girder Type	Section	Overall Height h (in)	Width b (in)	Steel Area $A_s=A'_s$ (in^2)	Effective Depth d (in)	Effective Depth d' (in)	Stirrups Area A_v (in^2)	Stirrups Spacing s (in)
Beam	A-A	48	36	7.11	44.5	20.5	0.40	12
	B-B	30	36	7.11	26.5	2.5	0.40	7
Pier	C-C	24	24	1.76	21.625	21.625	0.10	12

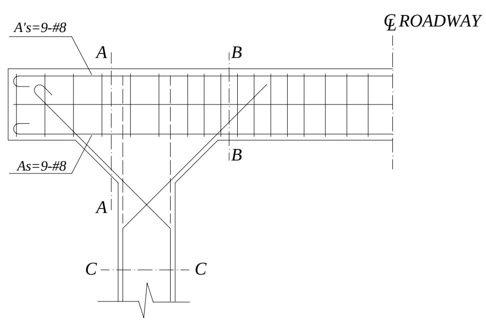

Figure 30 – Portion of the Bent

C.4.2 Positive Moment Strengthening

The beam flexural capacity is summarized in Table 19. No flexural strengthening is needed.

Table 19 – Positive Moment Flexural Capacity

Section (see Figure 30)	ϕM_n (k-ft)	M_u (k-ft)
Mid-span	536.7	495.2

C.4.3 Negative Moment Check

The beam does not need strengthening in its negative moment region. The as-built flexural capacity and flexural demand are summarized in Table 20 for the cross-section of interest.

Table 20 – Negative Moment Flexural Capacity

Section	Flexural Capacity ϕM_n (k-ft)	Flexural Demand M_u (k-ft)
A-A	1066.7	564.5
B-B	447.6	337.5

C.4.4 Shear Capacity Check

The beam does not need shear strengthening because the as-built shear capacity is acceptable as summarized in Table 21.

Table 21 – Beam Shear Capacity

Section	Shear Capacity ϕV_n (kip)	Shear Demand V_u (kip)
A-A	202.7	131.5
B-B	162.3	162.7

Shear capacity at Section B-B has been calculated using the detailed Eq. (11-5) (ACI 318-99) assuming M_u=*180 k-ft*.

C.4.5 Piers Check

Flexural and axial load capacities of the piers need not be upgraded because the ultimate moment and axial load demand is inside the P-M diagram of the members, as shown in Figure 31.

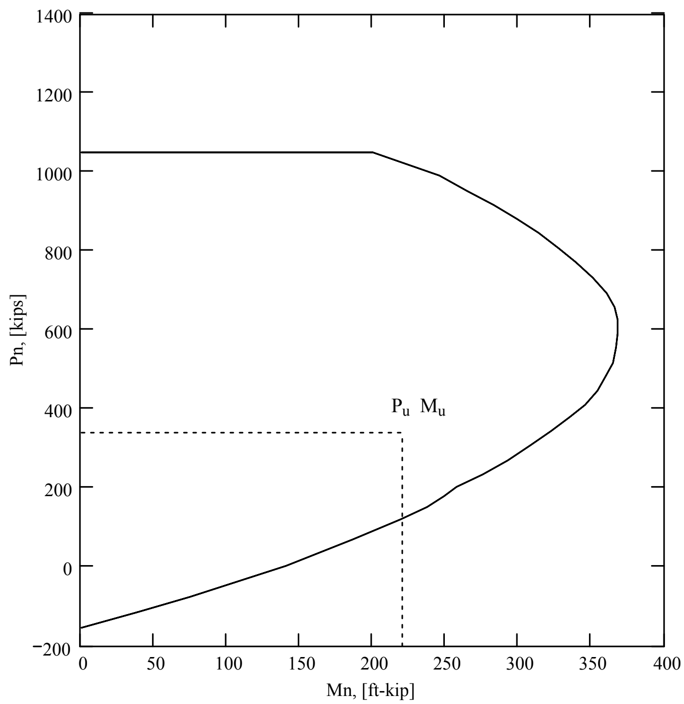

Figure 31 – Pier Flexural and Axial Load Capacity

D. LOAD RATING

Bridge load rating calculations provide a basis for determining the safe load carrying capacity of a bridge. According MoDOT, anytime a bridge is built, rehabilitated, or re-evaluated for any reason, inventory and operating ratings are required using the Load Factor rating method. All bridges should be rated at two load levels, the maximum load level called the Operating Rating and a lower load level called the Inventory Rating. The Operating Rating is the maximum permissible load that should be allowed on the bridge. Exceeding this level could damage the bridge. The Inventory Rating is the load level the bridge can carry on a daily basis without damaging the bridge.

In Missouri, for the Load Factor Method the Operating Rating is based on the appropriate ultimate capacity using current AASHTO specifications (AASHTO, 1994). The Inventory Rating is taken as 86% of the Operating Rating.

The method for determining the rating factor is that outlined by AASHTO in the Manual for Condition Evaluation of Bridges (AASHTO, 1996). Equation (12) was used:

$$RF = \frac{C - A_1 D}{A_2 L (1 + I)} \tag{12}$$

where: RF is the Rating Factor, C is the capacity of the member, D is the dead load effect on the member, L is the live load effect on the member, I is the impact factor to be used with the live load effect, A_1 is the factor for dead loads, and A_2 is the factor for live loads. Since the load factor method is being used, A_1 is taken as 1.3 and A_2 varies depending on the desired rating level. For Inventory rating, A_2 = 2.17, and for Operating Rating, A_2 = 1.3.

To determine the rating (RT) of the bridge Equation (13) was used:

$$RT = (RF)W \tag{13}$$

In the above equation, W is the weight of the nominal truck used to determine the live load effect.

For Bridge T-0530, the Load Rating was calculated for a number of different trucks, HS20, H20, 3S2, and MO5. The different ratings are used for different purposes by the bridge owner. For each of the different loading conditions, the maximum shear and maximum moment were calculated. An impact factor is also taken into account for load rating. This value for Bridge T-0530 is 29%. The live load effect of each truck on the different elements of the bridge was determined using the same methodology already described in the APPENDICES A-D.

D.1 Slab Rating

The shear and positive and negative moment values for the slab are shown below in Table 22.

Table 22 - Maximum Shear and Positive and Negative Moments due to Live Loads for the Central Span Slabs

Truck	Maximum Positive Moment [kip-ft/ft]	Maximum Negative Moment [kip-ft/ft]	Maximum Shear [kip/ft]	Maximum Positive Moment with Impact Factor [kip-ft/ft]	Maximum Negative Moment with Impact Factor [kip-ft/ft]	Maximum Shear with Impact Factor [kip/ft]
HS20	4.9	1.8	3.6	6.4	2.3	4.6
MO5	2.5	0.9	1.8	3.2	1.1	2.3
H20	2.5	0.9	1.8	3.2	1.1	2.3
3S2	2.5	0.9	1.8	3.2	1.1	2.3

Table 23, Table 24, Table 25 and Table 26 give the results of the Load Rating pertaining to positive moment strengthening with Type 2 and Type 3 strengthening techniques. The rating results for the negative moment regions are summarized in Table 27 while the results for the shear forces are shown in Table 28.

Table 23- Rating Factor for the Slabs at the Positive Bending Moment Regions (Zone A, Type 2 Strengthened)

Truck	Rating Factor (RF)	Rating (RT) (Tons)	Rating Type
HS20	1.400	50.4	Operating
HS20	0.839	30.2	Inventory
MO5	2.801	100.8	Operating
H20	2.409	48.2	Posting
3S2	2.409	88.2	Posting

* All Units Expressed in English System

Table 24 - Factor for the Slabs at the Positive Bending Moment Regions (Zone B, Type 2 Strengthened)

Truck	Rating Factor (RF)	Rating (RT) (Tons)	Rating Type
HS20	1.316	47.4	Operating
HS20	0.788	28.4	Inventory
MO5	2.632	94.7	Operating
H20	2.263	45.3	Posting
3S2	2.263	82.9	Posting

* All Units Expressed in English System

Table 25 - Rating Factor for the Slabs at the Positive Bending Moment Regions (Zone A, Type 3 Strengthened)

Truck	Rating Factor (RF)	Rating (RT) (Tons)	Rating Type
HS20	1.533	55.2	Operating
HS20	0.918	33.1	Inventory
MO5	3.066	110.4	Operating
H20	2.637	52.7	Posting
3S2	2.637	96.6	Posting

* All Units Expressed in English System

Table 26 - Factor for the Slabs at the Positive Bending Moment Regions (Zone B, Type 3 Strengthened)

Truck	Rating Factor (RF)	Rating (RT) (Tons)	Rating Type
HS20	1.328	47.8	Operating
HS20	0.796	28.6	Inventory
MO5	2.656	95.6	Operating
H20	2.284	45.7	Posting
3S2	2.284	83.7	Posting

* All Units Expressed in English System

Table 27 - Rating Factor for the Slab (Negative Bending Moments)

Truck	Rating Factor (RF)	Rating (RT) (Tons)	Rating Type
HS20	2.781	100.1	Operating
HS20	1.666	60.0	Inventory
MO5	5.562	200.2	Operating
H20	4.784	95.7	Posting
3S2	4.784	175.3	Posting

* All Units Expressed in English System

Table 28 - Rating Factor for the Slab (Shear)

Truck	Rating Factor (RF)	Rating (RT) (Tons)	Rating Type
HS20	1.420	51.1	Operating
HS20	0.851	30.6	Inventory
MO5	2.840	104.1	Operating
H20	2.443	48.9	Posting
3S2	2.443	89.5	Posting

* All Units Expressed in English System

D.2 Girders Rating

The bending moment values due to the live loads corresponding to the most critical sections for exterior and interior girders are summarized below in Table 29and Table 30 respectively. Table 31,

Table **32**, Table 33 and Table 34 summarize the corresponding rating factors.

Table 29 - Maximum Bending Moments due to the Live Loads at the Critical Positions for the Exterior Girders

	Bending Moment at the Critical Positions [kip-ft]				Bending Moment at the Critical Positions with Impact Factor [kip-ft]			
Position [in]	**HS20**	**MO5**	**H20**	**3S2**	**HS20**	**MO5**	**H20**	**3S2**
44.25	73.6	62.9	47.3	53.1	94.9	81.1	61.0	68.5
83.25	124.7	106.0	82.5	87.8	160.9	136.8	106.4	113.2
120	161.3	136.2	108.6	110.0	208.1	175.7	140.1	141.9
156	185.9	159.3	128.1	125.4	239.8	205.5	165.3	161.8
204	206.6	178.0	145.2	141.2	266.5	229.6	187.4	182.2
275	214.4	188.5	152.8	149.8	276.6	243.1	197.2	193.3

Table 30 Maximum Bending Moments due to the Live Loads at the Critical Positions for the Interior Girders

	Bending Moment at the Critical Positions [kip-ft]				Bending Moment at the Critical Positions with Impact Factor [kip-ft]			
Position [in]	**HS20**	**MO5**	**H20**	**3S2**	**HS20**	**MO5**	**H20**	**3S2**
44.25	134.8	115.2	86.7	97.3	173.9	148.6	111.8	125.5
83.25	228.6	194.2	151.2	160.8	294.9	250.6	195.0	207.5
120	295.5	249.5	199.0	201.6	381.2	321.9	256.7	260.1
156	340.5	292.0	234.7	229.8	439.3	376.6	302.8	296.5
204	378.5	326.1	266.1	258.7	488.3	420.6	343.3	333.8
275	392.9	345.3	280.0	274.5	506.8	445.4	361.3	354.1

Table 31 – Rating Factors for the Exterior Girders (Bending Moments, Type 2 Strengthening)

			Rating Factors RF_i Computed at the Critical Positions				
Position [in]	Un-factored Moment due to Dead Load [k-ft]	Moment Capacity [k-ft]	HS20	HS20	MO5	H20	3S2
44.25	135.9	639.0	3.746	2.244	4.385	4.457	4.457
83.25	236.0	923.3	2.948	1.766	3.468	3.253	3.253
120	313.4	1205.7	2.951	1.768	3.495	3.006	3.006
156	373.3	1205.7	2.311	1.384	2.498	2.148	2.148
204	428.7	1205.7	1.788	1.071	1.788	1.538	1.538
275	459.3	1388.2	1.722	1.032	1.722	1.481	1.481
Rating Factor: $RF = \min\{RF_i\}$			1.722	1.032	1.722	1.481	1.481
Rating (RT) [Tons]			62.00	37.14	63.11	29.62	54.27
Rating Type			Operating	Inventory	Operating	Posting	Posting

* All Units Expressed in English System

Table 32 – Rating Factors for the Exterior Girders (Bending Moments, Type 3 Strengthening)

			Rating Factors RF_i Computed at the Critical Positions				
Position [in]	Un-factored Moment due to Dead Load [k-ft]	Moment Capacity [k-ft]	**HS20**	**HS20**	**MO5**	**H20**	**3S2**
44.25	135.9	639.0	3.746	2.244	4.385	4.457	4.457
83.25	236.0	923.3	2.948	1.766	3.468	3.253	3.253
120	313.4	1205.7	2.951	1.768	3.495	3.006	3.006
156	373.3	1205.7	2.311	1.384	2.498	2.148	2.148
204	428.7	1205.7	1.788	1.071	1.788	1.538	1.538
275	459.3	1386.4	1.718	1.029	1.718	1.478	1.478
Rating Factor: $RF = \min\{RF_i\}$			1.718	1.029	1.718	1.478	1.478
Rating (RT) [Tons]			61.86	37.06	62.96	29.56	54.15
Rating Type			Operating	Inventory	Operating	Posting	Posting

* All Units Expressed in English System

Table 33 – Rating Factors for the Interior Girders (Bending Moments, Type 2 Strengthening)

			Rating Factors RF_i Computed at the Critical Positions				
Position [in]	Un-factored Moment due to Dead Load [k-ft]	Moment Capacity [k-ft]	HS20	HS20	MO5	H20	3S2
44.25	107.8	644.8	2.232	1.337	2.613	2.948	2.661
83.25	187.2	932.0	1.796	1.076	2.114	2.245	2.196
120	248.6	1218.5	1.807	1.082	2.140	2.126	2.126
156	296.1	1406.1	1.788	1.071	2.086	1.961	1.961
204	340.0	1567.8	1.774	1.063	2.059	1.775	1.775
275	364.3	1567.8	1.661	0.995	1.670	1.436	1.436
Rating Factor: $RF = \min\{RF_i\}$			1.661	0.995	1.670	1.436	1.436
Rating (RT) [Tons]			59.78	35.82	61.17	28.72	52.61
Rating Type			Operating	Inventory	Operating	Posting	Posting

* All Units Expressed in English System

Table 34 – Rating Factors for the Interior Girders (Bending Moments, Type 3 Strengthening)

			Rating Factors RF_i Computed at the Critical Positions				
Position [in]	Un-factored Moment due to Dead Load [k-ft]	Moment Capacity [k-ft]	**HS20**	**HS20**	**MO5**	**H20**	**3S2**
44.25	107.8	644.8	2.232	1.337	2.613	2.948	2.661
83.25	187.2	932.0	1.796	1.076	2.114	2.245	2.196
120	248.6	1218.5	1.807	1.082	2.140	2.126	2.126
156	296.1	1300.4	1.603	0.960	1.870	1.758	1.758
204	340.0	1480.7	1.636	0.980	1.900	1.637	1.637
275	364.3	1573.7	1.670	1.000	1.679	1.444	1.444
44.25	107.8	644.8	2.232	1.337	2.613	2.948	2.661
Rating Factor: $RF = \min\{RF_i\}$			1.603	0.960	1.679	1.444	1.444
Rating (RT) [Tons]			57.72	34.58	61.50	28.87	52.89
Rating Type			Operating	Inventory	Operating	Posting	Posting

* All Units Expressed in English System

The shear force values to the live loads corresponding to the most critical sections for exterior and interior girders are summarized below in Table 35

Table 35and
Table **36** respectively. Table 37 and
Table **38** summarize the corresponding rating factors.

Table 35 - Maximum Shear Forces due to the Live Loads at the Critical Positions for the Exterior Girders

	Shear Forces at the Critical Positions [kip]				Shear Forces at the Critical Positions with Impact Factor [kip]			
Position [in]	**HS20**	**MO5**	**H20**	**3S2**	**HS20**	**MO5**	**H20**	**3S2**
0	22.0	18.7	14.1	16.1	28.4	24.2	18.2	20.8
83.25	18.0	15.3	11.9	12.6	23.2	19.7	15.4	16.3
108	16.7	14.1	11.3	11.4	21.5	18.2	14.5	14.7
144	14.9	12.6	10.2	9.9	19.2	16.2	13.2	12.8
204	11.9	10.2	8.6	8.1	15.4	13.1	11.0	10.5
240	9.8	8.8	7.5	7.2	12.6	11.4	9.7	9.2
275	8.0	7.7	6.6	6.2	10.3	9.9	8.4	8.0

Table 36 - Rating Factors for the Exterior Girders (Shear Forces, Type 2 Strengthening)

	Shear Forces at the Critical Positions [kip]				Shear Forces at the Critical Positions with Impact Factor [kip]			
Position [in]	**HS20**	**MO5**	**H20**	**3S2**	**HS20**	**MO5**	**H20**	**3S2**
0	73.6	62.9	47.3	53.1	94.9	81.1	61.0	68.5
83.25	124.7	106.0	82.5	87.8	160.9	136.8	106.4	113.2
108	161.3	136.2	108.6	110.0	208.1	175.7	140.1	141.9
144	185.9	159.3	128.1	125.4	239.8	205.5	165.3	161.8
204	206.6	178.0	145.2	141.2	266.5	229.6	187.4	182.2
240	214.4	188.5	152.8	149.8	276.6	243.1	197.2	193.3
275	0.0	0.0	0.0	0.0	94.9	81.1	61.0	68.5

Table 37 – Rating Factors for the Exterior Girders (Shear Forces, Type 2 Strengthening)

			Rating Factors RF_i Computed at the Critical Positions				
Position [in]	Un-factored Moment due to Dead Load [k-ft]	Moment Capacity [k-ft]	HS20	HS20	MO5	H20	3S2
0	40.1	139.9	1.727	1.035	1.727	1.485	1.485
83.25	28.0	132.6	3.187	1.909	3.754	4.135	3.907
108	24.3	119.4	3.135	1.878	3.719	4.002	3.942
144	19.1	111.5	3.469	2.078	4.110	4.341	4.480
204	10.3	106.2	4.651	2.786	5.446	5.568	5.860
240	5.1	106.2	6.059	3.630	6.740	6.778	7.139
275	0.0	106.2	7.916	4.742	8.243	8.319	8.808
Rating Factor: $RF = \min\{RF_i\}$			1.727	1.035	1.727	1.485	1.485
Rating (RT) [Tons]			62.18	37.25	63.29	29.71	54.43
Rating Type			Operating	Inventory	Operating	Posting	Posting

* All Units Expressed in English System

Table 38 – Rating Factors for the Interior Girders (Shear Forces, Type 2 Strengthening)

			Rating Factors RF_i Computed at the Critical Positions				
Position [in]	Un-factored Moment due to Dead Load [k-ft]	Moment Capacity [k-ft]	HS20	HS20	MO5	H20	3S2
0	31.8	193.9	2.241	1.342	2.241	1.927	1.927
83.25	22.2	138.5	1.987	1.190	2.335	2.572	2.431
108	19.3	123.3	1.914	1.147	2.270	2.443	2.406
144	15.1	114.3	2.068	1.239	2.450	2.588	2.671
204	8.2	106.2	2.625	1.573	3.060	3.128	3.292
240	4.0	106.2	3.365	2.016	3.731	3.753	3.952
275	0.0	106.2	4.308	2.581	4.499	4.540	4.807
Rating Factor: $RF = \min\{RF_i\}$			1.914	1.147	2.241	1.927	1.927
Rating (RT) [Tons]			68.90	41.28	82.10	38.54	70.61
Rating Type			Operating	Inventory	Operating	Posting	Posting

* All Units Expressed in English System

D.3 Bents

Table 39 summarizes ultimate moments and shear forces calculated at four cross-sections where maximum values are reached.

Table 39 – Bending Moments and Shear Forces at the Critical Cross Sections

	Bending Moment at the Critical Positions [kip-ft/ft]				Shear Forces at the Critical Positions [kip-ft/ft]			
Sections	**HS20**	**H20**	**3S2**	**MO5**	**HS20**	**H20**	**3S2**	**MO5**
B-A	84.0	55.9	55.9	55.9	35.7	23.8	23.8	23.8
B-C	192.4	127.4	127.4	127.4	65.9	43.6	43.6	43.6
C-B	186.6	123.3	123.3	123.3	65.9	43.6	43.6	43.6
B-D	108.5	71.5	71.5	71.5	16.6	10.9	10.9	10.9

Table 40 - Rating Factors for the Bents (Bending Moments)

			Rating Factors RF_i Computed at the Critical Positions				
Sections	Un-factored Bending Moment due to Dead Load [k-ft]	Moment Capacity [k-ft]	**HS20**	**HS20**	**MO5**	**H20**	**3S2**
B-A	97.5	447.6	2.938	1.760	4.415	3.797	3.797
B-C	112.9	1066.7	3.678	2.203	5.554	4.777	4.777
C-B	69.3	536.7	1.841	1.103	2.786	2.396	2.396
B-D	15.4	350.0	2.339	1.402	3.550	3.053	3.053
Rating Factor: $RF = \min\{RF_i\}$			1.841	1.103	2.786	2.396	2.396
Rating (RT) [Tons]			66.28	39.71	102.09	47.92	87.80
Rating Type			Operating	Inventory	Operating	Posting	Posting

* All Units Expressed in English System

Table 41 - Rating Factors for the Bents (Shear Forces)

			Rating Factors RF_i Computed at the Critical Positions				
Sections	Un-factored Shear Forces due to Dead Load [kip]	Shear Capacity [kip]	**HS20**	**HS20**	**MO5**	**H20**	**3S2**
B-A	41.5	202.7	3.202	1.918	4.809	4.136	4.136
B-C	31.7	162.3	1.413	0.847	2.136	1.837	1.837
C-B	31.7	162.3	1.413	0.847	2.136	1.837	1.837
B-D	2.4	73.2	3.247	1.945	4.946	4.253	4.253
Rating Factor: $RF = \min\{RF_i\}$			1.413	0.847	2.136	1.837	1.837
Rating (RT) [Tons]			50.88	30.48	78.28	36.75	67.32
Rating Type			Operating	Inventory	Operating	Posting	Posting

* All Units Expressed in English System

D.4 Piers

Axial loads due to live loads and corresponding rating factors are summarized in Table 42 and Table 43.

Table 42 - Axial Loads due to Live Loads

Truck	Maximum Axial Load [kip]	Maximum Axial Load with Impact Factor [kip]
HS20	78.8	101.7
MO5	52.2	67.4
H20	52.2	67.4
3S2	52.2	67.4

Table 43 - Rating Factor for the Piers (Axial Loads)

Truck	Rating Factor (RF)	Rating (RT) (Tons)	Rating Type
HS20	4.441	159.9	Operating
HS20	2.660	95.8	Inventory
MO5	6.698	241.1	Operating
H20	5.761	115.2	Posting
3S2	5.761	211.1	Posting

* All Units Expressed in English System

D.5 Summary and Conclusions

The rating of the bridge is determined by the least rated element. Table 44 summarizes the rating of each element of the bridge. The most deficient element is the deck strengthened for positive moments with “Type 2” reinforcement.

Since the factors RF with which posting is determined are greater than 1 the bridge does not need to be load posted. In addition, from Table 44 the maximum operating and inventory load can be found as 47.4 T and 28.4 T respectively.

Table 44 – Summary of the rating of all the elements

	Rating Factors RF_E for the Elements				
Elements	**HS20**	**HS20**	**MO5**	**H20**	**3S2**
Slab: Positive Moments, Zone A, Type 2 Strengthened	1.4	0.839	2.801	2.409	2.409
Slab: Positive Moments, Zone B, Type 2 Strengthened	1.316	0.788	2.632	2.263	2.263
Slab: Positive Moments, Zone A, Type 3 Strengthened	1.533	0.918	3.066	2.637	2.637
Slab: Positive Moments, Zone B, Type 3 Strengthened	1.328	0.796	2.656	2.284	2.284
Slab: Negative Moments	2.781	1.666	5.562	4.784	4.784
Slab: Shear Forces	1.42	0.851	2.84	2.443	2.443
Exterior Girders: Bending Moments, Type 2 Strengthening	1.722	1.032	1.722	1.481	1.481
Exterior Girders: Bending Moments, Type 3 Strengthening	1.722	1.032	1.722	1.481	1.481
Interior Girders: Bending Moments, Type 2 Strengthening	1.661	0.995	1.67	1.436	1.436
Interior Girders: Bending Moments, Type 3 Strengthening	1.661	0.995	1.67	1.436	1.436
Exterior Girders: Shear Forces, Type 2 Strengthening	1.727	1.035	1.727	1.485	1.485
Interior Girders: Shear Forces, Type 2 Strengthening	1.914	1.147	2.241	1.927	1.927
Bents: Bending Moments	1.841	1.103	2.786	2.396	2.396
Bends: Shear Forces	1.413	0.847	2.136	1.837	1.837
Piers	4.441	2.66	6.698	5.761	5.761
Rating Factor: $RF = \min\left\{RF_E\right\}$	1.316	0.788	1.67	1.436	1.436
Rating (RT) [Tons]	47.376	28.37	61.19	28.72	52.62
Rating Type	Oper-ating	Inven-tory	Oper-ating	Post-ing	Post-ing

REFERENCES

[1] AASHTO, 2002: “Standard Specifications for Highway Bridges”, 17th Edition, Published by the American Association of State Highway and Transportation Officials, Washington D.C.
[2] ACI 440.2R-02, 2002: “Guide for the Design and Construction of Externally Bonded FRP Systems for Strengthening Concrete Structures,” Published by the American Concrete Institute, Farmington Hills, MI.
[3] AASHTO, 1998: “LRFD Bridge Design Specifications”, Second Edition, Published by the American Association of State Highway and Transportation Officials, Washington D.C.
[4] ACI 318-99, 1999: “Building Code Requirements for Structural Concrete and Commentary (318R-99),” Published by the American Concrete Institute, Farmington Hills, MI.
[5] AASHTO, 1996 “LRFD Design Code for Highway Bridges”, Published by the American Association of State Highway and Transportation Officials, Washington, D.C.
[6] AASHTO, 1994 “Manual for Condition Evaluation of Bridges”, Published by the American Association of State Highway and Transportation Officials, Washington, D.C.

APPENDIX A – Load Transfer and Slab Analysis

The statically indeterminate structure shown in Figure 7-*I* can be reduced to two simpler structures, as represented in Figure 32. R_2 and R_3 represent the unknowns of the problem to be determined by imposing the compatibility of the displacements as expressed in Eq. (14).

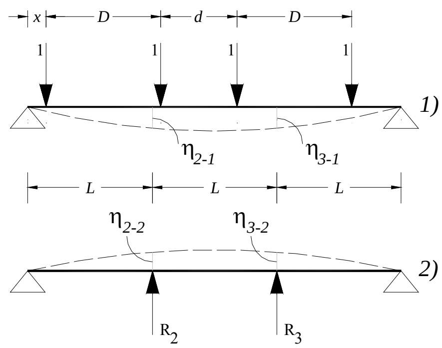

Figure 32 – Structures Equivalent to Figure 7-*I*

$$\begin{aligned} \eta_{2-1} &= \eta_{2-2} \\ \eta_{3-1} &= \eta_{3-2} \end{aligned} \tag{14}$$

By using superposition, Beam 1 and Beam 2 in Figure 32 are equivalent to the four beams shown in Figure 33, and to the two beams of Figure 34, respectively. The compatibility equation can be rearranged as follows for the first and second terms, respectively:

$$\begin{aligned} \eta_{2-1} &= \eta_{2-1a} + \eta_{2-1b} + \eta_{2-1c} + \eta_{2-1d} \\ \eta_{3-1} &= \eta_{3-1a} + \eta_{3-1b} + \eta_{3-1c} + \eta_{3-1d} \end{aligned} \tag{15}$$

$$\begin{aligned} \eta_{2-2} &= \eta_{2-2a} + \eta_{2-2b} \\ \eta_{3-2} &= \eta_{3-2a} + \eta_{3-2b} \end{aligned} \tag{16}$$

The second terms of Eqs. (15) and (16) can be expressed as shown in Eqs. (17), (18), and (19) respectively.

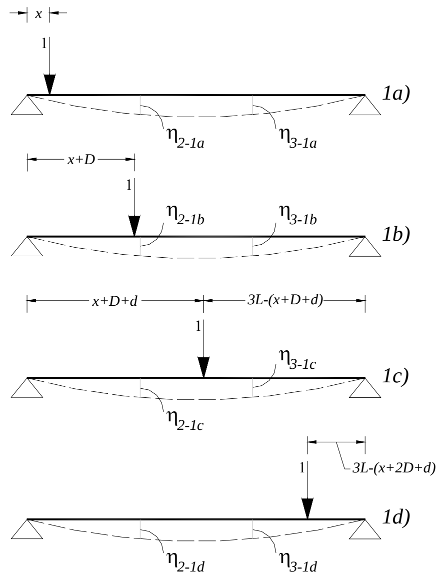

Figure 33 – Structures Equivalent to Beam 1 in Figure 32

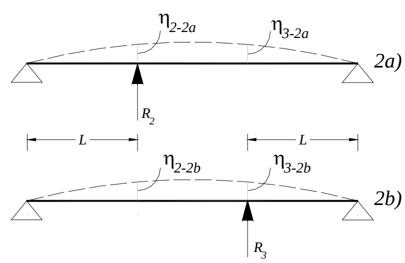

Figure 34 – Structures Equivalent to Beam 2 in Figure 32

$$
\begin{aligned}
\eta_{2-1a} &= \frac{x}{9}\left(5L^2 - x^2\right) \\
\eta_{2-1b} &= \frac{3L-(x+D)}{18}\left(8L^2 - \left(3L - \left(x+D\right)\right)^2\right) \\
\eta_{2-1c} &= \frac{3L-(x+D+d)}{18}\left(8L^2 - \left(3L - \left(x+D+d\right)\right)^2\right) \\
\eta_{2-1d} &= \frac{3L-(x+2D+d)}{9}\left(8L^2 - \left(3L - \left(x+2D+d\right)\right)^2\right)
\end{aligned}
\tag{17}
$$

$$
\begin{aligned}
\eta_{3-1a} &= \frac{x}{18}\left(8L^2 - x^2\right) \\
\eta_{3-1b} &= \frac{x+D}{18}\left(8L^2 - \left(x+D\right)^2\right) \\
\eta_{3-1c} &= \frac{3L-(x+D+d)}{9}\left(5L^2 - \left(3L - \left(x+D+d\right)\right)^2\right) \\
\eta_{3-1d} &= \frac{3L-(x+2D+d)}{9}\left(5L^2 - \left(3L - \left(x+2D+d\right)\right)^2\right)
\end{aligned}
\tag{18}
$$

$$
\begin{aligned}
\eta_{2-2a} &= \frac{4R_2L^3}{9EI} \\
\eta_{3-2a} &= \frac{7R_2L^3}{18EI} \\
\eta_{2-2b} &= \frac{7R_3L^3}{18EI} \\
\eta_{3-2b} &= \frac{4R_3L^3}{9EI}
\end{aligned}
\tag{19}
$$

By substituting the three previous equations into Eq. (14), the values of the vertical reactions R_2 and R_3 can be found. By knowing these two values, the other two vertical reactions, R_1 and R_4, shown in Figure 9, are easily determined by force equilibrium as follows:

$$
\begin{aligned}
R_1 &= \frac{12L - 4(x+D) - 2d - 2R_2L - R_3L}{3L} \\
R_4 &= 4 - (R_1 + R_2 + R_3)
\end{aligned}
\tag{20}
$$

Bending moment and shear force of this case can be found from the following Eqs. (21) and (22) (see Figure 35). It should be noted that the vertical reactions from Eq. (20), as well as R_1 and R_2, need to be multiplied by *P/2 (P=axle load)* because the previous analysis was conducted using unit forces.

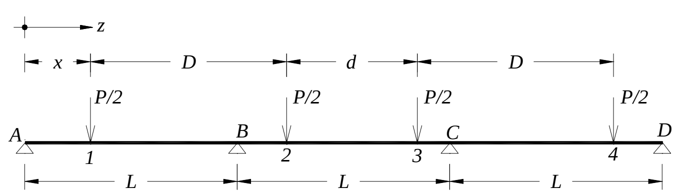

Figure 35 – Definitions for M and V (See Eqs. (21) and (22))

$$
\begin{aligned}
M_{A-1} &= R_1 z \\
M_{1-B} &= M_{A-1} - 0.5P(z-x) \\
M_{B-2} &= M_{1-B} + R_2(z-L) \\
M_{2-3} &= M_{B-2} - 0.5P[z-(x+D)] \\
M_{3-C} &= M_{2-3} - 0.5P[z-(x+D+d)] \\
M_{C-4} &= M_{3-C} + R_3(z-2L) \\
M_{4-D} &= M_{C-4} - 0.5P[z-(x+2D+d)]
\end{aligned}
\tag{21}
$$

$$
\begin{aligned}
V_{A-1} &= R_1 \\
V_{1-B} &= V_{A-1} - 0.5P \\
V_{B-2} &= V_{1-B} + R_2 \\
V_{2-3} &= V_{B-2} - 0.5P \\
V_{3-C} &= V_{2-3} - 0.5P \\
V_{C-4} &= V_{3-C} + R_3 \\
V_{4-D} &= V_{C-4} - 0.5P
\end{aligned}
\tag{22}
$$

The case shown in Figure 7-*II* is similar to the one already presented if:

$$
\eta_{2-1c} = \eta_{2-1d} = \eta_{3-1c} = \eta_{3-1d} = 0 \tag{23}
$$

and if R_1 and R_2 from Eq.(20) are replaced with:

$$
\begin{aligned}
R_1 &= \frac{6L-2x-D-2R_2L-R_3L}{3L} \\
R_4 &= \frac{2x+D-2R_3L-R_2L}{3L}
\end{aligned}
\tag{24}
$$

Bending moment and shear force for this second case can be written as follows:

$$
\begin{aligned}
M_{A-1} &= R_1 z \\
M_{1-B} &= M_{A-1} - 0.5P(z-x) \\
M_{B-2} &= M_{1-B} + R_2(z-L) \\
M_{2-C} &= M_{B-2} - 0.5P[z-(x+D)] \\
M_{C-D} &= M_{2-C} + R_3(z-2L)
\end{aligned}
\tag{25}
$$

$$\begin{aligned}
V_{A-1} &= R_1 \\
V_{1-B} &= V_{A-1} - 0.5P \\
V_{B-2} &= V_{1-B} + R_2 \\
V_{2-C} &= V_{B-2} - 0.5P \\
V_{C-D} &= V_{2-C} + R_3
\end{aligned} \tag{26}$$

APPENDIX B – Load lane Analysis

a) Distributed Load

As stated in AASHTO, the load lane load consists of *0.64 kip/ft*, uniformly distributed in the longitudinal direction. Transversely, it is uniformly distributed over a *10.0 ft* width. The share that each girder carries can be found by analyzing the structure shown in Figure 36.

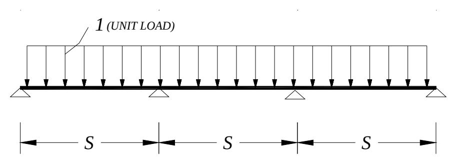

Figure 36 – Determination of k_ℓ

The beam represented in Figure 36 can be analyzed by studying the two simpler structures shown in Figure 37 when the following compatibility equation is met:

$$\begin{aligned} \eta_{2a} &= \eta_{2b} \\ \eta_{3a} &= \eta_{3b} \end{aligned} \tag{27}$$

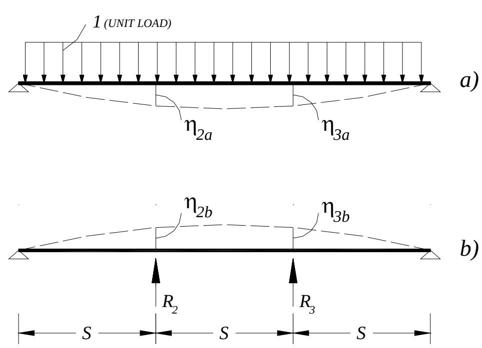

Figure 37 – Beams Equivalent to Figure 36

Considering symmetry of both geometry and loading, R_2=R_3=R, and therefore the second equation of Eq. (27) can be neglected. Furthermore, one can write:

$$\begin{aligned} \eta_{2a} = \eta_{3a} &= \frac{11}{12}\frac{1 \cdot S^4}{EI} \\ \eta_{2b} = \eta_{3b} &= \frac{15}{18}\frac{RS^3}{EI} \end{aligned} \tag{28}$$

and the unknown, R, can be found as follows:

$$R = \frac{11}{10} S = 1.1 \cdot S \tag{29}$$

Using equilibrium, the left and right vertical reactions (which are equal) of the beam shown in Figure 36 can be determined as being equal to *0.4S*. The values of k_L are *1.10* and *0.40* for interior and exterior girders, respectively.

b) Concentrated Load

The analysis related to the concentrated load being part of the Load Lane loading condition can be done on the simply supported bay laid out in Figure 38. The assumption is on the safe side because the remaining portion of the deck as depicted in Figure 36 is neglected.

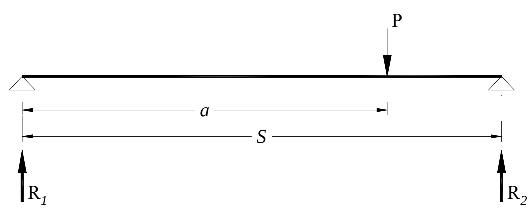

Figure 38 – Concentrated Load Analysis

The two vertical reactions, R_1 and R_2, can be written as follows:

$$\begin{aligned} R_1 &= \frac{P(S-a)}{S} \\ R_2 &= \frac{Pa}{S} \end{aligned} \tag{30}$$

Given both bridge and Load lane geometry the following reactions can be found for moment and shear analysis, respectively:

$$\begin{aligned} &R_1 = R_2 = 0.50P \quad (S = 78", a = 78"/2) \\ &R_1 = 0.23P,\ R_2 = 0.77P \quad (S = 78", a = 60") \end{aligned} \tag{31}$$

c) Combined

Ultimate unfactored moment and shear due to live loads can be written as follows:

$$
\begin{aligned}
M_u &= \frac{qL^2}{8} + k_\ell^{'} \frac{P_M L}{4} \\
V_u &= \frac{qL}{2} + k_\ell^{'} \frac{P_V (L-d)}{L}
\end{aligned}
\tag{32}
$$

where q is expressed by Eq. (4), L is the girder length, P_M*=18.0 kip* and P_V*=26.0 kip*, d is the girder effective depth, and $k_\ell^{'}$ is summarized in Table 45 for exterior and interior girders, respectively.

Table 45 – $k_\ell^{'}$ Coefficients

Coefficients	Loading Condition	Exterior Girder	Interior Girder
$k_\ell^{'}$	Moment	0.50	0.50
	Shear	0.23	0.77

It is to be noted that the maximum bending moment is obtained by placing the concentrated load at mid-span, and the maximum shear force by placing the concentrated load at a distance d from the support.

APPENDIX C – Girder Analysis for an HS20-44 Truck

As previously recognized, girder analysis is carried out by taking into consideration only three of the five cases corresponding to five different positions of the design truck load on the single span, as shown in Figure 13. The first case of Figure 13 is enlarged in Figure 39.

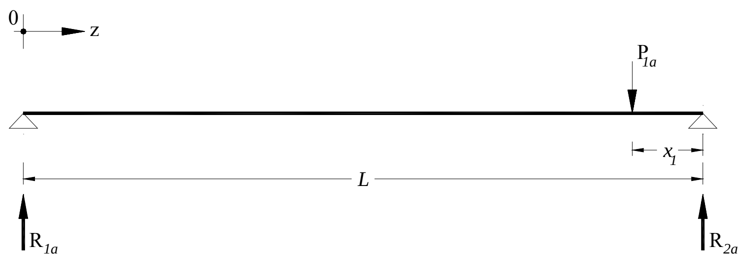

Figure 39 – One Wheel Load on the Girder

Vertical reactions R_1 and R_2 are defined as follows:

$$R_{1a} = P_{1a} - R_{2a}$$
$$R_{2a} = \frac{P_{1a}(L - x_1)}{L} \tag{33}$$

Shear and moment diagrams can be expressed as a function of *z* as follows:

$$V_a(z) = \begin{cases} R_{1a} & if \quad z \le L - x_1 \\ R_{1a} - P_{1a} & otherwise \end{cases}$$
$$M_a(z) = \begin{cases} R_{1a} z & if \quad z \le L - x_1 \\ R_{1a} z - P_{1a}[z - (L - x_1)] & otherwise \end{cases} \tag{34}$$

The second case (Figure 13*b)* is shown in Figure 40. Vertical reactions are:

$$R_{1b} = P_{1a} + P_{1b} - R_{2b}$$
$$R_{2b} = R_{2a} + \frac{P_{1b}(L - x_1 + L_{1a})}{L} \tag{35}$$

Shear and moments can be written as:

$$V_b(z) = \begin{cases} R_{1b} \quad if \quad z \le L - x_1 \\ R_{1b} - P_{1a} \quad if \quad L - x_1 \le z \le L - x_1 + L_{1a} \\ R_{1b} - P_{1a} - P_{1b} \quad otherwise \end{cases}$$

$$M_b(z) = \begin{cases} R_{1b} z \quad if \quad z \le L - x_1 \\ R_{1b} z - P_{1a}[z - (L - x_1)] \quad if \quad L - x_1 \le z \le L - x_1 + L_{1a} \\ R_{1b} z - P_{1a}[z - (L - x_1)] + P_{1b}[z - (L - x_1 + L_{1a})] \quad otherwise \end{cases} \tag{36}$$

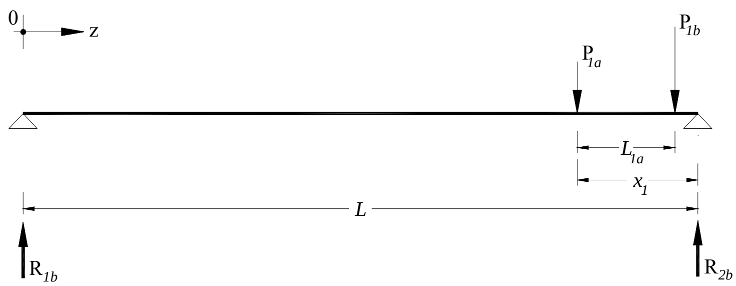

Figure 40 – Two Wheel Loads on the Girder

When three wheel loads are present on the girder (see Figure 41), vertical reactions are expressed as follows:

$$\begin{aligned} R_{1c} &= P_{1a} + P_{1b} + P_{1c} - R_{2c} \\ R_{2c} &= R_{2b} + \frac{P_{1c}(L - x_1 + L_{1a} + L_{1b})}{L} \end{aligned} \tag{37}$$

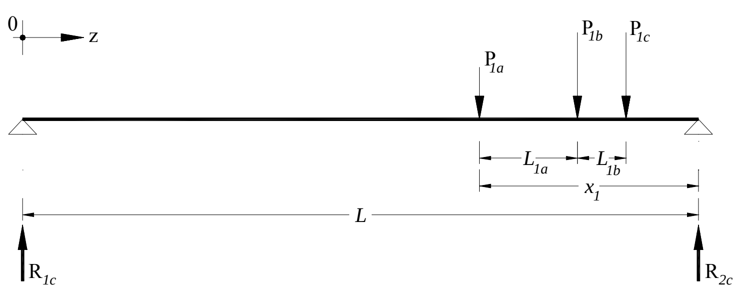

Figure 41 – Three Wheel Loads on the Girder

Shear and moments can be written as follows:

$$V_c(z)=\begin{cases} R_{1c} \quad if \quad z \le L-x_1 \\ R_{1c}-P_{1a} \quad if \quad L-x_1 \le z \le L-x_1+L_{1a} \\ R_{1c}-P_{1a}-P_{1b} \quad if \quad L-x_1+L_{1a} < z < L-x_1+L_{1a}+L_{1b} \\ R_{1c}-P_{1a}-P_{1b}-P_{1c} \quad otherwise \end{cases}$$

$$M_c(z)=\begin{cases} R_{1c}z \quad if \quad z \le L-x_1 \\ R_{1c}z-P_{1a}[z-(L-x_1)] \quad if \quad L-x_1 \le z \le L-x_1+L_{1a} \\ R_{1c}z-P_{1a}[z-(L-x_1)]-P_{1b}[z-(L-x_1+L_{1a})] \quad if \quad L-x_1+L_{1a} < z < L-x_1+L_{1a}+L_{1b} \\ R_{1c}z-P_{1a}[z-(L-x_1)]-P_{1b}[z-(L-x_1+L_{1a})]-P_{1c}[z-(L-x_1+L_{1a}+L_{1b})] \ otherwise \end{cases} \tag{38}$$

APPENDIX D – Bent Analysis

The bent, represented in Figure 19 can be considered equivalent to the two structures shown in Figure 42 as soon as:

$$M = P_1(a - x) \tag{39}$$

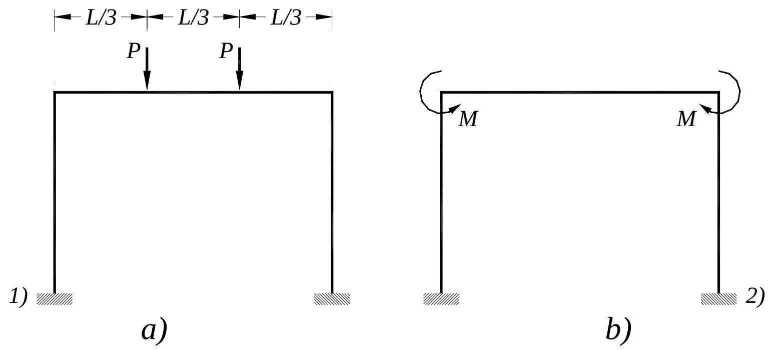

Figure 42 – Bent Equivalent Structures (Live Load)

This loading condition needs to be completed by adding the one due to the dead load of the structure. This case is presented immediately after the live load analysis.

Frames shown in Figure 42 can be simplified in the four structures laid out in Figure 43 when compatibility is satisfied, so that:

$$\begin{aligned} \alpha_{1a} &= \alpha_{1b} \\ \alpha_{2a} &= \alpha_{2b} \end{aligned} \tag{40}$$

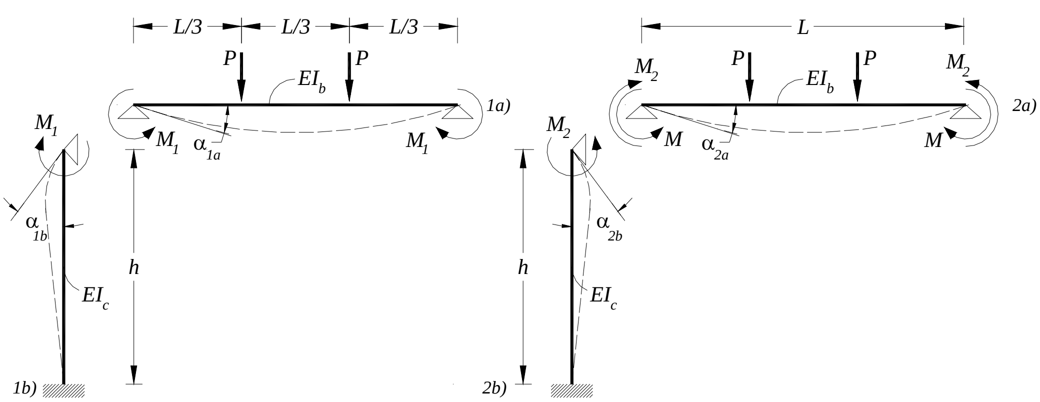

Figure 43 – Frames Equivalent to Figure 42

The four terms in Eq.(40) can be expressed as follows:

$$\begin{aligned}
\alpha_{1a} &= \frac{PL^2}{9EI_b} - \frac{M_1 L}{2EI_b} \\
\alpha_{1b} &= \frac{M_1 h}{4EI_c} \\
\alpha_{2a} &= -\frac{ML}{2EI_b} + \frac{M_2 L}{2EI_b} \\
\alpha_{2b} &= -\frac{M_2 h}{4EI_c}
\end{aligned} \tag{41}$$

By replacing Eq. (41) in Eq. (40) M_1 and M_2 can be found as follows:

$$\begin{aligned}
M_1 &= \frac{4PL^2 I_c}{9(2LI_c + hI_b)} \\
M_2 &= \frac{2MLI_c}{2LI_c + hI_b}
\end{aligned} \tag{42}$$

Using superposition, bending moments for the frame of Figure 19 can be found as follows:

$$\begin{aligned}
M_{B-A} &= M \\
M_{B-C} &= M_1 + M - M_2 \\
M_{C-B} &= \frac{PL}{4} - M_1 - (M - M_2) \\
M_{B-D} &= M_1 - M_2 \\
M_{D-B} &= -\frac{M_1 - M_2}{2}
\end{aligned} \tag{43}$$

Shear forces and moments due to self weight of the bent can be calculated in a similar fashion by looking at the two structures represented in Figure 44 and imposing the compatibility equation as follows:

$$\alpha_{1D} = \alpha_{2D} \tag{44}$$

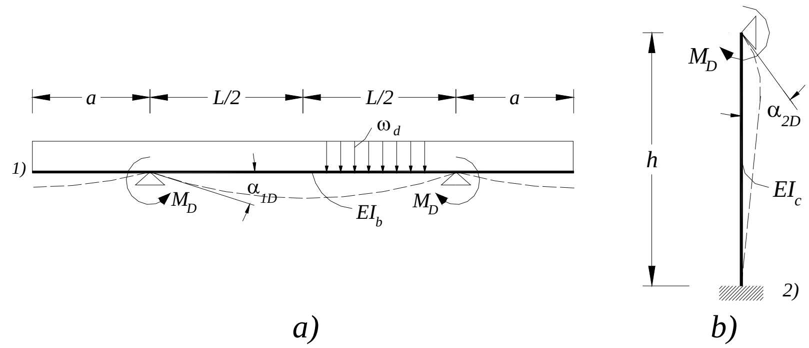

Figure 44 – Equivalent Bent Structures (Dead Load)

The structure of Figure 44*b* is identical to the structure of Figure 43-*2b*, while the one shown in Figure 44*a* can be simplified into the one of Figure 45*a)* where *M*** equals the following:

$$M^{**} = M_D + \frac{\omega_d a^2}{2} \tag{45}$$

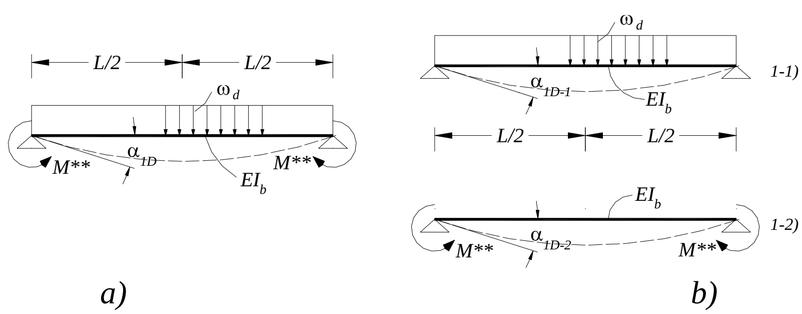

Figure 45 – Structures Equivalent to the Beam of Figure 44*a*

Figure 45*a)*, in turn, can be replaced by the two beams of Figure 45*b)*. By satisfying Eq. (44), the unknown M_D can be found as follows:

$$M_D = \frac{\omega_d L(L^2 - 6a^2) I_c}{6(I_b h + 2I_c L)} \tag{46}$$